This is the author-formatted version of Peti et al., 2017, Palaeogeography, Palaeoclimatology, Palaeoecology 468, 142-161, http://dx.doi.org/10.1016/j.palaeo.2016.12.004

Sinemurian–Pliensbachian calcareous nannofossil biostratigraphy and organic carbon isotope stratigraphy in the Paris Basin: calibration to the ammonite biozonation of NW Europe

Leonie Peti[a,†], Nicolas Thibault[a,*], Marie-Emilie Clémence[b], Christoph Korte[a], Jean-Louis Dommergues[c], Cédric Bougeault[c], Pierre Pellenard[c], Mads Engholm Jelby[d], Clemens V. Ullmann[e]

[a] *Department of Geosciences and Natural Resource Management, University of Copenhagen, Øster Voldgade 10, DK-1350 Copenhagen K, Denmark*
[b] *University of Innsbruck, Institute of Geology, Faculty of Geo- and Atmospheric Sciences, Innrain 52, Innsbruck 6020, Austria*
[c] *Biogeosciences, UMR CNRS/uB 6282, Univ. Bourgogne Franche-Comté, 6 Boulevard Gabriel, 21000 Dijon, France*
[d] *Natural History Museum of Denmark, University of Copenhagen, Øster Voldgade 5-7, DK-1350 Copenhagen K, Denmark*
[e] *University of Exeter, Camborne School of Mines & Environment and Sustainability Institute, Penryn Campus, Penryn, Cornwall TR10 9FE, U.K.*
** Corresponding author. Tel.: +45 35 32 33 50, E-mail address: nt@ign.ku.dk (N. Thibault). Department of Geosciences and Natural Resource Management, University of Copenhagen, Øster Voldgade 10, DK-1350 Copenhagen K, Denmark*
† Current address: School of Environment, University of Auckland, PB 92019, 23 Symonds Street, Auckland, New Zealand

Abstract: The biostratigraphy of Sinemurian to lower Toarcian calcareous nannofossils has been investigated in the Sancerre-Couy core (Paris Basin), which contains a mixed assemblage of species with affinities to the northern and southern areas of the peritethyan realm, thus allowing for the use and calibration of the Mediterranean Province (Italy/S France) and NW Europe (UK) biozonation schemes. This study is based on semi-quantitative analyses of the calcareous nannofossil assemblage performed on 145 samples and the recorded bioevents are calibrated to the NW European Ammonite Zonation and to a new organic carbon isotope curve based on 385 data points. The main bioevents, i.e. the first occurrences of Parhabdolithus liasicus, Crepidolithus pliensbachensis, Crepidolithus crassus, Mitrolithus lenticularis, Similiscutum cruciulus sensu lato, Lotharingius hauffii, Crepidolithus cavus and Lotharingius sigillatus as well as the last occurrence of Parhabdolithus robustus, have been identified. However, we show that a large number of standard biostratigraphic markers show inconsistent occurrences at the base and top of their range, possibly accounting for some of the significant discrepancies observed between the different domains. In addition to the nine main bioevents used for the biozonation of the core, we document an additional 50 distinct bioevents, evaluate their reliability and discuss their potential significance by comparison to previous studies. A total of five significant negative organic carbon isotope excursions are identified and defined in the Paris Basin including the well-documented Sinemurian–Pliensbachian boundary event. One positive excursion is further defined in the Pliensbachian interval. Our calibration of high-resolution calcareous nannofossil biostratigraphy to ammonite biostratigraphy and organic carbon isotopes represents a new stratigraphic reference for the Lower Jurassic series.

1. Introduction

The Early Jurassic marks the first major evolutionary burst of coccolithophorids. Although the oldest coccolithophorids are dated as Late Triassic (Carnian according to Bown et al., 2004 and Erba, 2006; and latest Norian according to Gardin et al., 2012), this group spread rapidly across oceans and experienced one of its most important radiation events during the Early Jurassic (Bown et al., 2004). The sharply rising abundance and diversity of calcareous nannofossils in Early Jurassic basins led to their use as excellent biostratigraphic markers for dating post-Triassic–Jurassic boundary sediments (Bown and Cooper, 1998; Mattioli and Erba, 1999; Veiga de Oliveira et al., 2007; Perilli et al., 2010; Mattioli et al., 2013; Fraguas et al., 2015).

Existing calcareous nannofossil biostratigraphic schemes correlate calcareous nannofossil zones to ammonite standard zonations of NW Europe and the Mediterranean Realm (Italy, South France and Portugal). The calibration of these respective schemes is not always easy due to ammonoid provincialism

(Page, 2003), and/or to the scarcity of ammonites in some intervals (Mattioli and Erba, 1999). Calcareous nannofossils, as well as ammonites, show provincialism resulting in the establishment of distinct nannofossil biostratigraphic schemes for NW Europe (Bown, 1987; reconsidered in Bown and Cooper, 1998), the Mediterranean Realm of Italy and South France (Mattioli and Erba, 1999), more recently the upper Sinemurian to lower Toarcian of the Lusitanian Basin (Mattioli et al., 2013) and of the Cantabrian Range (Fraguas et al., 2015). Re-evaluation of taxonomic descriptions, mostly of the genera Similiscutum (de Kænel and Bergen, 1993), Biscutum (Mattioli et al., 2004b), Crepidolithus (Fraguas and Erba, 2010) and Lotharingius (Mattioli, 1996; Fraguas and Young, 2011) has allowed the erection of revised and updated schemes for the SE Mediterranean realm (Mattioli et al., 2013) and the Cantabrian Range/N Spain (Fraguas et al., 2015, 2016).

Despite the existence of a precise calibration of calcareous nannofossil zonations to ammonite biostratigraphy in the aforementioned studies, significant discrepancies in the position and in the successive order of bioevents remain between different domains of the peri-tethyan realm. Moreover, many studies focus on the late Pliensbachian and lower Toarcian time intervals (Mailliot et al., 2007, 2013; Veiga de Oliveira et al., 2007; Fraguas et al., 2008, 2015; Boulila et al., 2014; Clémence et al., 2015) whereas only the recent studies of Mattioli et al. (2013) and Plancq et al. (2016) extend into the upper Sinemurian. The focus on calcareous nannofossil response to late Pliensbachian–early Toarcian palaeo-environmental perturbations (Perilli, 2000; Bucefalo Palliani et al., 1998, 2002; Mattioli et al., 2004a, 2008, 2009; Tremolada et al., 2005; Mailliot et al., 2006, 2007, 2009; Bour et al., 2007; Veiga de Oliveira et al., 2007; Suan et al., 2010; Fraguas and Young, 2011; Fraguas et al., 2012) has driven the attention away from lower parts of the Lower Jurassic and data are still limited for the Sinemurian to lower Pliensbachian time interval (Mattioli et al., 2013; Fraguas et al., 2015). The demonstration of large-scale, potentially greenhouse-icehouse climatic changes (Dera et al., 2011; Korte and Hesselbo, 2011; Silva and Duarte, 2015) and large carbon isotopic excursions prior to the early Toarcian Oceanic Anoxic Event (eT–OAE) (van de Schootbrugge et al., 2005; Korte and Hesselbo, 2011; Riding et al., 2013; Duarte et al., 2014; Franceschi et al., 2014; Silva and Duarte, 2015; Gomez et al., 2016; Plancq et al., 2016) call for the establishment of a refined stratigraphy of the whole Sinemurian–Pliensbachian interval. Intensifying the focus on the Sinemurian is also essential to improve the biostratigraphy during the earliest significant evolutionary steps of calcareous nannoplankton. Although the aforementioned studies have demonstrated the existence of a number of carbon isotope excursions in the Sinemurian–Pliensbachian of the Tethys, no attempt to calibrate both ammonite and nannofossil biostratigraphy to high-resolution carbon isotope stratigraphy has yet been undertaken for the entire upper Sinemurian to basal Toarcian interval.

The investigated Sancerre-Couy core spans the complete Lower Jurassic and has a reasonably well-established ammonite biozonation for the upper Sinemurian–Pliensbachian (Degouy et al., 1986; Lorenz, 1987; Lorenz et al., 1988; Gély and Lorenz, 1991; Lorenz and Gély, 1994; Boulila et al., 2014). Situated in the Paris Basin, the studied core represents an area located between the NW European and SE and SW Mediterranean realms, hence allowing for comparison of the different established biostratigraphic schemes.

This paper focuses on the calcareous nannofossil distribution from the base of the Sinemurian to lower Toarcian of the Sancerre-Couy core and aims at establishing a precise biostratigraphy of this interval, revising the ammonite zonation, and at calibrating both biozonations to a new high-resolution organic carbon isotope curve. Comparison of our results to previously established biostratigraphic schemes allows for a comprehensive overview of the Sinemurian to lower Toarcian calcareous nannofossil biostratigraphy at the scale of the western peri-tethyan domain.

2. Geological setting and previous work on the Sancerre-Couy core

Concomitant with the break-up of the supercontinent Pangaea in the Early Jurassic, an epicontinental seaway in NW Europe opened as part of the Western Tethys Ocean (Fig. 1; Bassoulet and Baudin, 1994; Hermoso et al., 2009). The Paris Basin was a sub-basin of the wide north-European epicontinental shelf which was characterized by marl-limestone alternations and silty shales (Jenkyns, 1988; Baudin et al., 1990; Gély and Lorenz, 1991; Hallam, 1997; Mattioli et al., 2008; Hermoso et al., 2009). This basin was located at a palaeolatitude of approximately 30°N and was part of the NW European lower shelf during the Early Toarcian (Gély and Lorenz, 1991; Bassoulet et al., 1993; Röhl et al., 2001; Ruebsam et al., 2014). The process of widespread drowning of carbonate platforms allowed hemipelagic conditions to settle in, supplemented by the development of relatively deep-water carbonates on subsided

continental margins (Hermoso et al., 2009). Sample material of this study was collected in summer 2012 and originates from the Sancerre-Couy core (GPF-Sancerre; 40°1'10.8''N, 2°47'6''E) drilled in the southernmost part of the Paris Basin (Fig. 1) in 1986-1987. Petrophysical data logging (gamma-ray and sonic) along with a sequence stratigraphic interpretation and a relative sea-level curve have previously been reported by Gély and Lorenz (1991) (Fig. 2). A large number of ammonite occurrences and the corresponding ammonite zonation of the core are gathered from the previous works of Degouy et al. (1986), Lorenz (1987), Lorenz et al. (1987, 1988) and Boulila et al. (2014). A detailed sedimentology of the core has been presented by Lorenz (1987) and Lorenz et al. (1987). The new sedimentological log is in agreement with the previous results of Lorenz but is slightly more detailed according to our observations during logging of the core which are reported on Figure 2. During the sampling process, it was observed that the length of the logged core from 348 to 447 m matched well reported core depths from the previous works of Lorenz (1987) and Lorenz et al. (1987). However, in the interval between 447.25 and 516 m, more core material was retrieved in core boxes than expected from the reported depths of several boxes, probably due to core dilation after drilling. The core was described in this interval with continuous depth. An adjusted core depth was assigned to each original core depth provided on core boxes in the

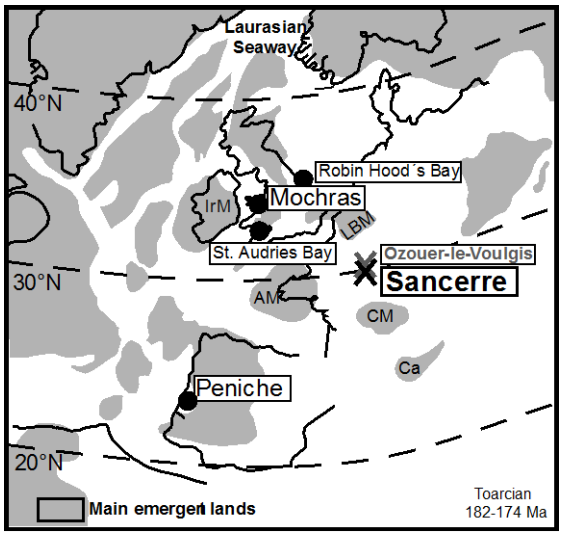

Figure 1: Palaeogeographical map for the Early Jurassic (Toarcian) of NW Europe. The black X marks the location of the Sancerre-Couy borehole. Modified after Bassoulet et al. (1993). Emerged lands are in white (LBM: London–Babant Massif, AM: Armorican Massif, CM: Central Massif, IrM: Irish Massif, Ca: Calabria).

interval between 447.25 and 516 m This results in a minor offset of 3.66 m between the two scales at the bottom of the core. The equivalence between original core depths and adjusted core depths is provided in Appendix A.

3. Methods

3.1. Calcareous nannofossils

A total of 145 samples, with an average stratigraphic resolution of 1.2 m, spanning the uppermost Hettangian to the lowermost Toarcian (ca. 200-182 Ma), were processed for calcareous nannofossil analysis, thus resulting in a temporal resolution of ca. 130 kyr per sample increment. All samples were carefully disaggregated and 150 mg (±0.5 mg) of dry sediment were dispersed in 50 mL of distilled water. The suspension was homogenised with a magnetic stirrer. Only in rare cases it was necessary to treat the suspension in an ultrasonic bath which was limited to no more than 15 s to prevent disaggregation of the delicate calcareous nannofossils. An aliquot of 0.75 mL of that suspension was spread evenly on a microscopic cover slip using a micropipette and dried slowly before mounting on a microscopic slide with a Norland optical adhesive. Thibault et al. (2012) and Koch and Young (2007) describe similar methods and have proved high reproducibility yielding a minimal error margin for counting absolute calcareous nannofossil abundances. The recent study of Bordiga et al. (2015) further confirms that the simple technique used here provides high-reproducibility and allows for calibration to other techniques commonly used to calculate absolute nannofossil abundances. Semi-quantitative counts of calcareous nannofossil species were performed with a LEICA DM750P light microscope at a magnification of 1600X (x100 oil objective with a x1.6 additional lens and x10 oculars). Following Thibault et al. (2015), a species were classified as abundant (A) if more than 10 specimens were observed in a field of view (FOV); common (C) if 1-10 specimens were observed in a FOV; frequent (F) if one specimen or more were observed in every 10 FOVs; rare (R) if only one specimen was observed in 11-100 FOVs; very rare (VR) if only one specimen was observed in 100-200 FOVs; single (S) if only one specimen was observed during the complete investigation (approximately 300 FOVs). The first and last occurrences (FOs and LOs) have been used, but as described below, many taxa show inconsistent records at the base (and sometimes at the top) of their range. In order to provide a quantitative biostratigraphy as precise as possible, we chose to define first consistent and last consistent occurrences (FCOs and LCOs; Appendix B), respectively at the base and top of stratigraphic intervals where species are not absent in more

than two contiguous samples. Acme events have also been considered when taxa were showing a significant and consistent change from frequent to common. Due to mixed NW Europe and Mediterranean calcareous nannofossil assemblages in the Sancerre-Couy core (see also Boulila et al., 2014), both biozonations of Bown and Cooper (1998) for NW Europe (NJ zonation) and of Mattioli and Erba (1999) recently revised by Mattioli et al. (2013) for the Mediterranean provinces (NJT zonation) have been applied. The applied taxonomic concepts follow Perch-Nielsen (1985) and Bown (1987). Calcareous nannofossil species considered in this text are listed in Appendix C. Preservational issues did not always allow the differentiation between the subspecies Parhabdolithus liasicus liasicus and P. liasicus distinctus. Therefore, these are both combined in Parhabdolithus liasicus despite distinct potential stratigraphic occurrences of the two sub-species. Following Mattioli et al. (2004), Similiscutum avitum, Similiscutum cruciulus, and Similiscutum orbiculus are here considered different ecophenotypes of the same species that have been grouped into 'S. cruciulus sensu lato' .

Preservation of the calcareous nannofossil assemblage was evaluated using the etching and overgrowth criteria of Roth (1983) on the coccoliths. Preservation of the assemblage was considered as good (G) if etching (E) and overgrowth (O) were not beyond stage 1 (E1 or O1), moderate (M) if either etching or overgrowth was reaching stage 2 (E2 or O2), and poor (P) if either etching or overgrowth was reaching stage 3 (E3 or O3). A fourth category (very poor, or VP) was considered here for assemblages characterized by stages E3/O3 and with a species richness ≤3 (Appendix B). Samples containing very few coccoliths and characterized by stages E4/O4 were considered as nearly barren (NB). A number of samples were completely barren of coccoliths (B).

3.2. Organic carbon isotopes

A total of 385 organic carbon isotope measurements with an average stratigraphic resolution of 43 cm were carried out at the Department of Geosciences and Natural Resource Management, University of Copenhagen, Denmark. Powdered samples were decarbonated by treatment with 10% HCl and washed with deionized water. Dried decarbonated powder equivalent to ~50 μg organic carbon was transferred into tin capsules. These capsules were combusted in a Euro EA Elemental Analyzer. Resulting CO2 was purified and transferred via chromatographic columns into a Micromass Iso-Prime triple collector mass spectrometer. Carbon isotope ratios were standardized using the inhouse standard AK (δ13CAK = −25.3 ‰) and expressed as per mille (‰) deviation from the Vienna Pee Dee Belemnite (VPDB) standard. The heterogeneity of the material was addressed by multiple analyses of single sample horizons. Observed δ13Corg ranges from these repeated analyses of seven horizons are 0.6 ‰ or smaller (average = 0.4 ‰; n = 2-5) except for two anomalous results deviating by −1.2 and −1.5 ‰ from the respective average value. Signal noise related to sample heterogeneity is expected to be the most important parameter generating fluctuations without a regional meaning in the δ13Corg record of the Sancerre-Couy core.

4. Results

4.1. Revision of the ammonite biozonation of the Sancerre-Couy core

The ammonite biozonation of the whole Sancerre-Couy core was presented in various papers following the original description of the core (Degouy et al., 1986; Lorenz et al., 1987, 1988, 1991; Gély and Lorenz, 1991; Lorenz and Gély, 1994). None of these papers provide a synthetic and comprehensive description of all ammonite specimens found with their precise depth. For our interval of interest, Lorenz et al. (1987) have provided a detailed biozonation of the uppermost Sinemurian to lower Toarcian. A few ammonite findings are given in detail by the latter authors, but predominantely only the depth of the bases and tops of ammonite zones are reported.

J. Lorenz kindly provided us the original list of the exact ammonite specimens found with their depth in the core which is reported here in Appendix D. In addition, data by I. Rouget in Boulila et al. (2014) and a number of new ammonites collected during our logging and identified by J. L. Dommergues (this study) are also reported (Appendix D). These additions allow for a moderate revision of the ammonite biozonation of the Sinemurian–lower Toarcian time interval in the Sancerre-Couy core. As in all previously cited references on the Sancerre-Couy core, this biozonation is based on first and last occurrences of ammonite index species.

4.1.1. Sinemurian

Most of the Sinemurian is devoid of ammonoids. However, the correlation of logging tools and deduced sequential boundaries between Sancerre-Couy and the Ozouer-le-Voulgis core, situated further North in the Paris Basin (Fig. 1) and containing few Sinemurian ammonites, allowed the establishment of a number of additional ammonite zones in the Sinemurian of Sancerre-Couy, such as the

Semicostatum AZ which projects between 496 and 492 m (ca. 498-494 m in our adjusted depth scale). Similarly, the correlation of Sancerre-Couy to Ozouer-le-Voulgis allows the assignment of a ca. 1.5-m-thick interval directly below the base of the Raricostatum AZ to the Oxynotum AZ (at 453-451.60 m; Fig. 2). The top of the Semicostatum AZ and base of the Oxynotum AZ remain elusive (Fig. 2). The Raricostatum AZ is identified in the core through the presence of numerous Echioceras sp. between 451.60 and 441.60 m. The interval comprised between 441.60 and 430.50 m does not contain any ammonoids and in consequence is unzoned. The Sinemurian–Pliensbachian boundary lies within this unzoned interval (Fig. 2). In this study, the compilation of ammonite occurrences suggests a slightly modified zonation as compared to the biozones originally defined by Lorenz et al. (1987) (Fig. 2). The latter authors chose to place the Sinemurian–Pliensbachian boundary, and hence the base of the Jamesoni Zone at 440 m, which corresponds to the aforementioned unzoned interval between the Raricostatum and Jamesoni AZs in this study (Fig. 2). This choice was driven by the correlation of stratigraphic sequences between Sancerre-Couy and other drill sites and sections of the Paris Basin as later presented in Gély and Lorenz (1991).

4.1.2. Pliensbachian

The base of the Jamesoni AZ originally defined at 440 m is placed here further up, corresponding to the coincident FO of Platypleuroceras sp. and Uptonia jamesoni at 430.50 m (Fig. 2). The top of the Jamesoni AZ is placed at the LO of U. jamesoni at 429.10 m and the following interval between 429 and 422.60 m, devoid of ammonoids, is unzoned. The base of the Ibex AZ is placed at the FO of Acanthopleuroceras sp. (422.60 m), which lies just below the FO of Acanthopleuroceras cf. A. maugenesti at 422 m (Fig. 2). The latter ammonoid bioevent is characteristic of the Valdani ammonite subzone (ASz), which comprises approximately half of the Ibex AZ in its middle part (Dommergues and Mouterde, 1981; Sapunov and Metodiev, 2007). This suggests that the base of the Ibex AZ may lie well below 422 m, somewhere within the 429-422.60 m unzoned interval. The FO of Aegoceras capricornus at 414.50 m is used to define the base of the Davoei AZ, as this species is characteristic of this zone. The 412 to 410 m interval yielded a diversified assemblage with numerous specimens of the Aegoceras lineage and two specimens of Prodactylioceras gr. davoei, characteristic of the Davoei AZ. The top of the Davoei AZ was originally placed by Lorenz et al. (1987) at 409 m, though this level did not deliver any ammonite specimen. This appears justified as this level is halfway between the LO of Prodactylioceras gr. davoei at 410 m and the FO of Amaltheus stokesi at 408.30 m. The latter ammonoid bioevent, together with the following FO of Protogrammoceras sp. at 407.50 m, are characteristic of the Stokesi ASz, which corresponds to the lower part of the Margaritatus AZ (Howarth, 1992). The position of the top of the Stokesi ASz is unclear in the original description by Lorenz et al. (1987) and no mention of the Subnodosus Asz is given by these authors. The finding of a last specimen of Amaltheus cf. A. stokesi at 394.50 m is tentatively used here to mark the LO of the species, thus defining the top of the Stokesi and base of the Subnodosus ASzs at 394.50 m. The base of the Gibbosus ASz is placed at the FO of Amaltheus gibbosus at 374.90 m, which is the marker for this subzone. Lorenz et al. (1987) originally placed the top of the Margaritatus AZ at 366.80 m and the Spinatum AZ between 366.80 and 355.50 m without any further justification of characteristic ammonite occurrences. The top of the Margaritatus AZ is justified by the LO of A. margaritatus at 366.90 m and the subsequent FO of Pleuroceras cf. P. solare at 366.20 m (Appendix D) which defines the base of the Spinatum AZ (Fig. 2). Several specimens of P. spinatum have been found up to 358.50 m confirming the assignment of this overall interval to the Spinatum AZ. The LO of P. solare at 355.80 m further suggests that this interval corresponds to the lower half of the Spinatum AZ as the latter species is characteristic of the Solare ASz which is equivalent to the Apyrenum ASz in NW Europe, i.e. the first subzone of the Spinatum AZ (Dommergues and Mouterde, 1981; Sapunov and Metodiev, 2007). No ammonites characteristic of the Hawskerense ASz have been found in the core.

4.1.3. Toarcian

The FO of Dactylioceras gr. tenuicostatum-semicelatum defines the base of the Tenuicostatum AZ at 352.80 m (Fig. 2). Together with the presence of a clear ravinement in the sediments at 355.05 m, these data suggest that the uppermost Pliensbachian and Pliensbachian–Toarcian (Pl–To) transition of the Sancerre-Couy core are characterized by an important hiatus. In contrast to the previous studies of Lorenz et al. (1987), Gély and Lorenz (1991) and Lorenz and Gély (1994), the position of the Pliensbachian–Toarcian boundary remains uncertain here within the unzoned interval at 355.80-352.80 m (Fig. 2). The FO of Dactylioceras gr. tenuicostatum-semicelatum at 352.80 m, immediately followed by that of D. semicelatum

at 352.40 m, are characteristic of the Semicelatum ASz, the last subzone of the Tenuicostatum AZ in the Boreal subzonation. Therefore, it is likely that a large part of the Tenuicostatum AZ is also missing due to the Pl–To hiatus. This interpretation is also supported by the thinness of this zone (ca. 4.8 m as compared to the 10.5 m thickness of the truncated Spinatum AZ). For the remaining lower Toarcian presented here, the base of the Serpentinum AZ at 348.00 m has already been justified by the new ammonite data reported by I. Rouget in Boulila et al. (2014).

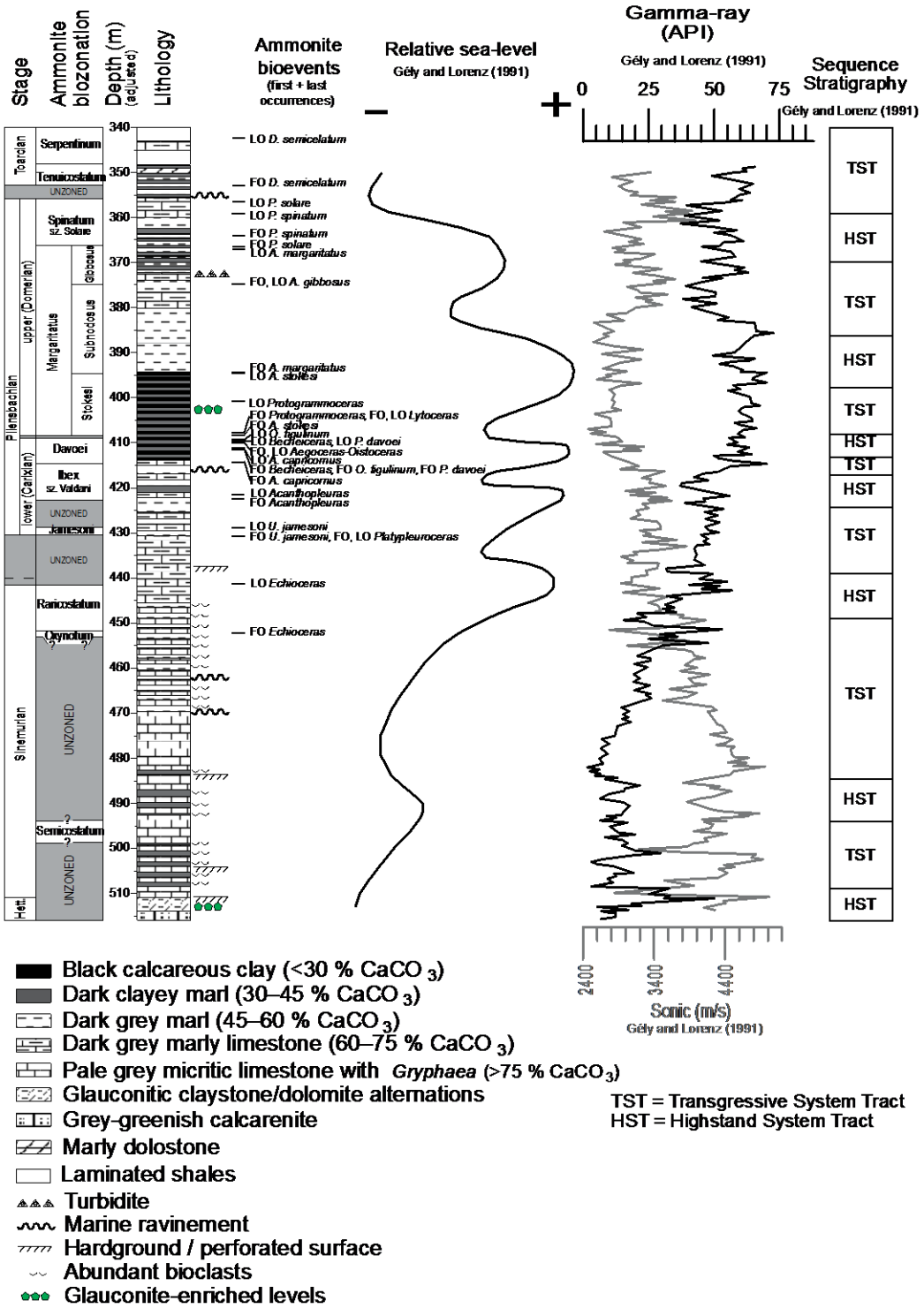

Figure 2: Revised ammonite zonation of the Sancerre-Couy core along with the lithology (this study), gamma-ray and sonic logs, relative sea-level curve and sequence stratigraphic interpretation of Gély and Lorenz (1991).

4.2. Calcareous nannofossil ranges and bioevents

The abundance and preservation of the investigated calcareous nannofossil assemblages differ profoundly throughout the record, with a general increase in both parameters from the bottom to the top of the core (Appendix B; Fig. 3). The abundance of lower Sinemurian calcareous nannofossil assemblages is very low and generally shows inconsistent occurrences (Fig. 3). Additional difficulties arise from the overall poor preservation of the few specimens observed in lower Sinemurian samples that prevented their identification (Appendix B). Therefore, the biostratigraphy of the lower Sinemurian is biased by the poor preservation of the assemblage.

The range of calcareous nannofossil species encountered in this study has been ordered according to their first occurrences (Fig. 3). Apparent major origination events are recorded in two intervals, both of which are associated with a distinct increase in abundance of the entire nannofossil assemblage, i.e. in the mid-Sinemurian around 470 m and in the uppermost Sinemurian around 445 m (Fig. 3). Fewer bioevents are recorded in the lower Pliensbachian (Carixian), whereas another long-lasting origination event characterizes the Margaritatus AZ of the upper Pliensbachian (Domerian) (Fig. 3). Few events have been recorded for the remaining part of the Pliensbachian and lowermost Toarcian and we have reported here the major bioevents, mostly dominated by LO events of the lower Toarcian (Fig. 4) as described in Boulila et al. (2014).

A detailed description of all calcareous nannofossil bioevents is furnished in Appendix E, and we summarize here the most important ones in Figure 3.

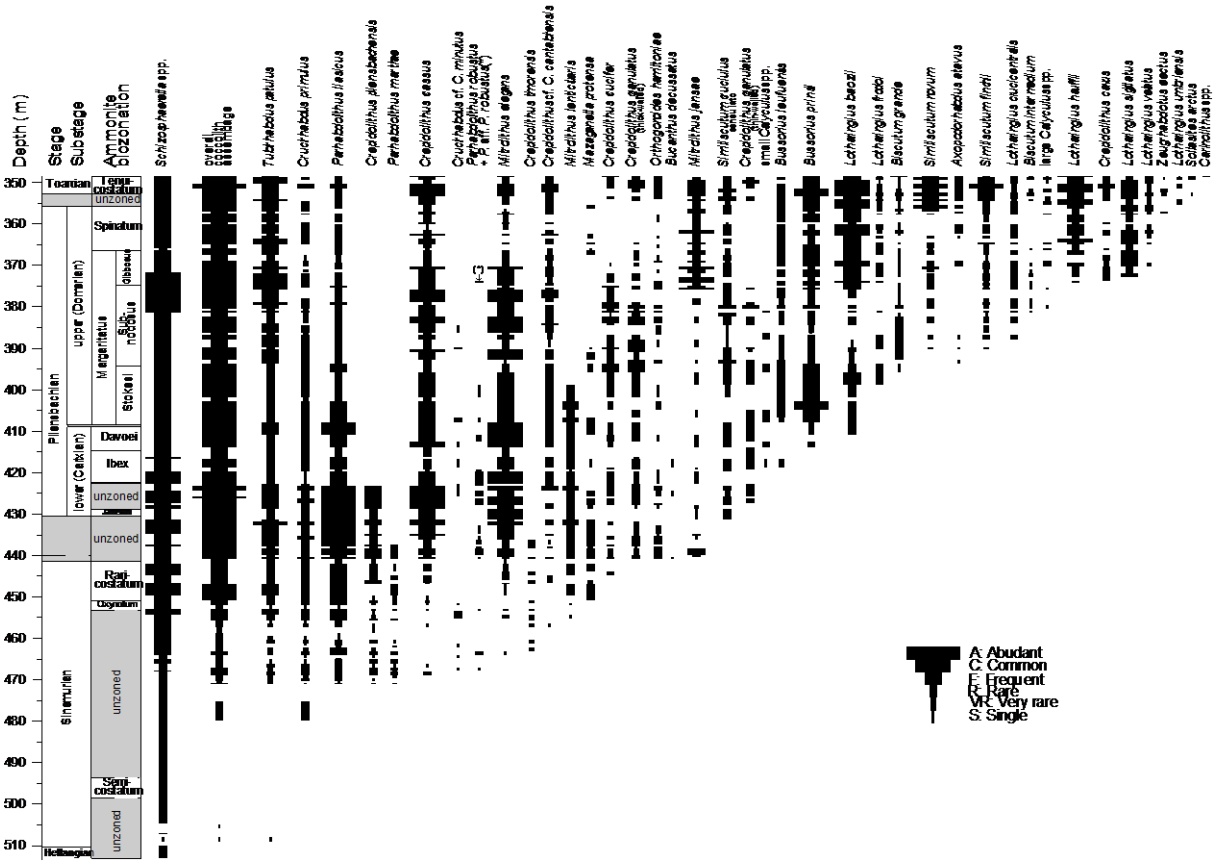

Figure 3: Semi-quantitative abundances of the overall calcareous nannofossil assemblage and recorded species of the Sancerre-Couy core. A: abundant (=>10 spp./FOV), C: common (=1-10spp./FOV), F: frequent(=1spp./1-10FOVs), R: rare(=1spp./10-100FOVs), VR: very rare(=1spp./101-299FOVs), S: single (=1spp./300FOVs). (*) indicates Parhabdolithus aff. P. robustus (see Appendix E for further explanation).

Only the nannolith (incertae sedis) Schizosphaerella spp. is present in the lowermost studied sample at 513.10 m in the uppermost Hettangian. The record of this taxon in the lowermost part of the Sinemurian is patchy before it remains present throughout the succession. The intervals from just below the Oxynotum AZ to the lower part of the Ibex AZ and the upper part of the Subnodosus ASz to the lower part of the Gibbosus ASz are characterized by higher abundances of Schizosphaerella spp. (Fig. 3). The succeeding FO of Tubirhabdus patulus is located at 509.10 m. No coccolith could

be identified below this level. This interval is uncertain in terms of ammonite biozonation but is situated right above the Hettangian–Sinemurian boundary (508.20 m or 511.00 m in the adjusted scale) as identified through lithostratigraphy and correlation of logging tools through the Paris Basin by Gély and Lorenz (1991) (Fig. 2). The FO of T. patulus is followed by a long interval of absence and subsequently, a FCO of this species can be placed at 471.10 m in the mid-Sinemurian coincident with the first occurrence of three other coccolith species (Parhabdolithus liasicus, Crepidolithus pliensbachensis, Parhabdolithus marthae) marking a general FCO of coccoliths (Fig. 3, 4). Both the FO and FCO of T. patulus as well as the FCO of coccoliths at 471.10 m mark local events, which appears as a sudden response to a change toward favourable environmental conditions allowing coccolithophorids to thrive. It is noticeable that this change occursduring the major transgression of the Sinemurian as shown in Gély and Lorenz (1991) (Fig. 2). The Sinemurian–Pliensbachian boundary transition is marked by the FOs of thick-walled Crepidolithus granulatus, Orthogonoides hamiltoniae, Bucanthus decussatus, Mitrolithus jansae and the base acme of P. liasicus, within the same interval of 50 cm between 440.80 and 440.30 m (Fig. 3). The FOs of Lotharingius umbriensis and Sollasites arctus and the FCO of Similiscutum novum mark the unzoned, transitional interval between the uppermost Pliensbachian (Spinatum AZ) and the basal Toarcian (Tenuicostatum AZ) (Fig. 3). A summary of all recorded calcareous nannofossil bioevents is provided in Table 1

Table 1: Nannofossil bioevents.

Nannofossil bio-events	Stage	Substage	Ammonite Zone	Ammonite Sz	depth (m)	Reliability
FO *Carinolithus* spp.	Toarcian	lower	Tenuicostatum	Semicelatum	348.6	robust
FO *Sollasites arctus*	?		unzoned		353.4	robust
FCO *Similiscutum novum*	?		unzoned		354.5	robust
FO *Lotharingius umbriensis*	?		unzoned		355.5	reliable
LO *Mazaganella protensa*	Pliensbachian	upper	Spinatum	Solare/Apyrenum	356.4	dubious
FCO *Axopodorhabdus atavus*	Pliensbachian	upper	Spinatum	Solare/Apyrenum	357.4	robust
FO *Zeugrhabdotus erectus*	Pliensbachian	upper	Spinatum	Solare/Apyrenum	357.4	dubious
base increase *Lotharingius hauffii*	Pliensbachian	upper	Margaritatus	Gibbosus	367.4	robust
FO *Lotharingius velatus*	Pliensbachian	upper	Margaritatus	Gibbosus	370.3	dubious
FO *Lotharingius sigillatus*	Pliensbachian	upper	Margaritatus	Gibbosus	372.8	robust
FO *Crepidolithus cavus*	Pliensbachian	upper	Margaritatus	Gibbosus	373.8	robust
FO *Lotharingius hauffii*	Pliensbachian	upper	Margaritatus	Gibbosus	374.1	robust
FCO *Mitrolithus jansae*	Pliensbachian	upper	Margaritatus	Subnodosus	375.8	robust
FO large *Calyculus* spp.	Pliensbachian	upper	Margaritatus	Subnodosus	380.4	dubious
FO *Biscutum intermedium*	Pliensbachian	upper	Margaritatus	Subnodosus	381.4	reliable
LO Crucirhabdus cf. C. minutus	Pliensbachian	upper	Margaritatus	Subnodosus	386.3	dubious
FO *Lotharingius crucicentralis*	Pliensbachian	upper	Margaritatus	Subnodosus	387.9	reliable
FO *Similiscutum finchii*	Pliensbachian	upper	Margaritatus	Subnodosus	390.3	robust
FO *Axopodorhabdus atavus*	Pliensbachian	upper	Margaritatus	Subnodosus	393.8	dubious
FO *Similiscutum novum*	Pliensbachian	upper	Margaritatus	Subnodosus	393.8	reliable
FO *Biscutum grande*	Pliensbachian	upper	Margaritatus	Stokesi	395.8	robust
FO *Lotharingius frodoi*	Pliensbachian	upper	Margaritatus	Stokesi	398.8	robust
LO *Mitrolithus lenticularis*	Pliensbachian	upper	Margaritatus	Stokesi	401.8	robust
LO *Parhabdolithus robustus*	Pliensbachian	upper	Margaritatus	Stokesi	401.8	dubious
FO *Lotharingius barozii*	Pliensbachian	lower	Davoei		410.8	robust
FO *Bussonius prinsii*	Pliensbachian	lower	Davoei		413.8	robust
FO *Bussonius leufuensis*	Pliensbachian	lower	Ibex		418.8	dubious
FO small *Calyculus* spp.	Pliensbachian	lower	Ibex		418.8	reliable
LCO *Parhabdolithus robustus*	Pliensbachian	lower	Ibex		419.8	robust
top acme *Parhabdolithus liasicus*	Pliensbachian	lower	unzoned		424.3	robust
LO *Crepidolithus pliensbachensis*	Pliensbachian	lower	unzoned		424.3	robust
FO thin-walled *Crepidolithus granulatus*	Pliensbachian	lower	unzoned		427.3	reliable
FO *Similiscutum cruciulus* sensu lato*	Pliensbachian	lower	unzoned/Jamesoni		431.3	reliable
LO *Crepidolithus timorensis*	Pliensbachian	lower	unzoned/Jamesoni		437.3	reliable
LO *Parhabdolithus marthae*	Pliensbachian	lower	unzoned/Jamesoni		437.8	robust
FO *Mitrolithus jansae*	Pliensbachian	lower	unzoned/Jamesoni		440.3	reliable
base acme *Parhabdolithus liasicus*	Pliensbachian	lower	unzoned/Jamesoni		440.8	robust
FO thick-walled *Crepidolithus granulatus*	Pliensbachian	lower	unzoned/Jamesoni		440.8	robust
FO *Orthogonoides hamiltoniae*	Pliensbachian	lower	unzoned/Jamesoni		440.8	reliable
FO *Bucanthus decussatus*	Pliensbachian	lower	unzoned/Jamesoni		440.8	dubious
FCO *Parhabdolithus robustus*	Pliensbachian	lower	unzoned/Jamesoni		440.8	robust
FO *Crepidolithus crucifer*	Sinemurian		Raricostatum		444.9	dubious
FCO *Mitrolithus lenticularis*	Sinemurian		Raricostatum		444.9	robust
FCO *Crepidolithus crassus*	Sinemurian		Raricostatum		446.7	robust
FCO *Mitrolithus elegans*	Sinemurian		Raricostatum		449.8	robust
FO *Mazaganella protensa*	Sinemurian		Raricostatum		450.7	robust
FO *Mitrolithus lenticularis*	Sinemurian		unzoned		455.3	dubious
FO *Crepidolithus cf. C. cantabriensis*	Sinemurian		unzoned		457.3	dubious
FO *Crepidolithus timorensis*	Sinemurian		unzoned		463.1	dubious
FO *Mitrolithus elegans*	Sinemurian		unzoned		464.1	dubious
FO *Crucirhabdus* cf. *C. minutus*	Sinemurian		unzoned		467.8	dubious
FO *Parhabdolithus robustus*	Sinemurian		unzoned		467.8	dubious
FO *Crepidolithus crassus*	Sinemurian		unzoned		468.8	dubious
FO *Parhabdolithus marthae*	Sinemurian		unzoned		471.1	local event
FCO *Tubirhabdus patulus*	Sinemurian		unzoned		471.1	local event
FCO coccolithus	Sinemurian		unzoned		471.1	local event
FO *Crepidolithus pliensbachensis*	Sinemurian		unzoned		471.1	local event
FO *Parhabdolithus liasicus*	Sinemurian		unzoned		471.1	local event
FO *Crucirhabdus primulus*	Sinemurian		unzoned		479.9	local event
FO *Tubirhabdus patulus*	Sinemurian		unzoned		509.1	local event
presence *Schizosphaerella* spp.	Hettangian		unzoned		513.1	local event

* comprising ecophenotypes: *Similiscutum avitum*, *Similiscutum cruciulus* and *Similiscutum orbiculus*
bold: zonal marker events

4.3. Calcareous nannofossil biozonation of the Sancerre-Couy core

The biozonations NJ and NJT defined by Bown and Cooper (1998) and Mattioli and Erba (1999), respectively, have been applied in this study using the FOs and LOs of zonal markers (Figs. 4, 5).

The top of NJ1 and NJT1 zones cannot be defined in this record due to the very small number of coccoliths present at the base of the studied interval (Fig. 4). Only the nannolith Schizosphaerella spp., the coccolith species T. patulus, Crucirhabdus primulus, and a few non-identified badly preserved coccoliths have been observed within the lower Sinemurian.

The NJT2 Parhabdolithus liasicus Zone defined from the FO of P. liasicus to the FO of C. pliensbachensis cannot be identified here as these two species first occur at the same depth. The NJ2 Zone whose top is defined by the FO of Crepidolithus crassus spans only a 2.3 m interval situated ca. 18 m below the base of the Oxynotum AZ. It is likely that only the topmost part of the NJ2 Zone is identified with certainty in our record, the whole lower Sinemurian interval below the FCO of coccoliths at 471.10 m being impossible to date with nannofossil biostratigraphy due to the scarcity of coccoliths in that interval. Furthermore, the FOs of P. marthae and C. pliensbachensis are located at the base of this zone. No subdivision of the NJ2 Zone is possible here (see below).

The NJ3 and NJT3 Crepidolithus crassus zones have their tops defined by the FO of Similiscutum cruciulus in the non-dated interval just below the Jamesoni AZ (Fig. 4). The FOs of Parhabdolithus robustus, Crucirhabdus cf. C. minutus, Mitrolithus elegans, Crepidolithus timorensis, Crepidolithus cf. C. cantabriensis, Mitrolithus lenticularis, Mazaganella protensa, Crepidolithus crucifer, C. granulatus, O. hamiltoniae, B. decussatus and M. jansae as well as the FCOs of M. elegans, C. crassus, P. robustus, the LOs of P. marthae and C. timorensis and the base of the acme event of P. liasicus are all recorded within this zone. The subdivision of the NJT3 Zone into the NJT3a Crepidolithus pliensbachensis Subzone and the NJT3b Mitrolithus lenticularis Subzone is possible here and placed at the FO of M. lenticularis, a few meters below the identified Oxynotum AZ (Fig. 4).

The NJ4/NJT4 Similiscutum cruciulus Zone has its top at the FO of Lotharingius hauffii within the lowermost part of the Gibbosus ASz of the Margaritatus AZ (Fig. 4). The FOs of the thin-walled C. granulatus, Bussonius leufuensis, small Calyculus spp., Bussonius prinsii, Lotharingius barozii, Lotharingius frodoi, Biscutum grande, S. novum, Axopodorhabdus atavus, Similiscutum finchii, Lotharingius crucicentralis, Biscutum intermedium and large Calyculus spp. as well as the LCO of P. robustus, the LOs of C. pliensbachensis, M. lenticularis and C. cf. C. minutus, the FCO of M. jansae and the top of the acme event of P. liasicus have been recorded in this zone. The subdivision of the NJ4/NJT4 Zones into NJ4a/NJT4a subzones and NJ4b/NJT4b subzones can be applied here. The top of the NJ4a/NJT4a subzones is defined by the LO of P. robustus and located within the Stokesi ASz of the Margaritatus AZ in both the NJ and NJT standard zonations (Fig. 7). In the Sancerre-Couy core, the rare occurrences of P. aff. P. robustus within the top of the Margaritatus AZ at 374.10 m correspond either to reworking of P. robustus, or to specimens of Parhabdolithus zweilii, a species which is considered as a synonym of P. robustus by Bown (1987) but as a distinct, valid species ranging up to the base Toarcian by E. de Kænel (pers. comm., 2016). The considered LO of P. robustus is thus at 401.80 m. However, the LO of this species is not reliable in the Sancerre-Couy core as it is preceded by a very patchy single occurrences (Fig. 3; Table 1). On the contrary, a distinctive LCO for this species has been found within the Ibex AZ, similar to its LO in standard zonations and to recent results of Fraguas et al. (2015) in the Basque-Cantabrian Basin. It is likely that the patchy occurrences of this species observed above the Ibex AZ in the Sancerre-Couy core correspond to reworking and that the LCO of the species at 419.80 m correlates to its LO as observed in other oceanic basins. Although no distinctive sign of reworking has been observed in the sediments, our interpretation is supported by the position of the LO of C. pliensbachensis in the Sancerre-Couy core below the Ibex AZ, just below the LCO of P. robustus. The LO of C. pliensbachensis is considered as a good secondary marker for the top of NJ4a and NJT4a in standard zonations (Fig. 7).

The FO of Carinolithus superbus (marked with * in Fig. 4) as identified in Sancerre-Couy by Boulila et al. (2014) defines the top of the NJ5 and NJT5 Lotharingius hauffii Zone within the Serpentinum AZ at 347.12 m. The subdivision of the NJ5 Zone into the NJ5a Biscutum finchii and the NJ5b Crepidolithus impontus subzones, based on the FO of Crepidolithus impontus (synonymous to Crepidolithus cavus), is located in the lowermost NJ5 Zone as this species first occurs in the sample immediately above the FO of L. hauffii (Fig. 4; Table 1). In the Sancerre-Couy core, the subdivision of the NJT5 Zone, using the FO of Lotharingius sigillatus that defines the base of the NJT5b Subzone, is located in the upper part of the Margaritatus AZ, near the base of the Gibbosus ASz, immediately above the previously

This is the author-formatted version of Peti et al., 2017, Palaeogeography, Palaeoclimatology, Palaeoecology 468, 142-161, http://dx.doi.org/10.1016/j.palaeo.2016.12.004

defined base of the NJ5b Subzone (Fig. 4; Table 1). The subdivisions of NJ5 and NJT5 appear concordant but result in very condensed NJ5a and NJT5a subzones (Fig. 4). The FOs of Lotharingius velatus, Zeugrhabdotus erectus, L. umbriensis, S. arctus and Carinolithus spp., the FCOs of A. atavus and S. novum, the LO of M. protensa as well as the 'base increase L. hauffii' have been recorded in the NJ5/NJT5 zones (Fig. 4; Table 1). Additionally, Boulila et al. (2014) recorded the LOs of C. primulus and C. (M.) jansae (marked with * in Fig. 4) in this zone.

The LOs of B. grande and P. liasicus have been recorded by Boulila et al. (2014) in the lower NJ6/NJT6 Zone (Fig. 4).

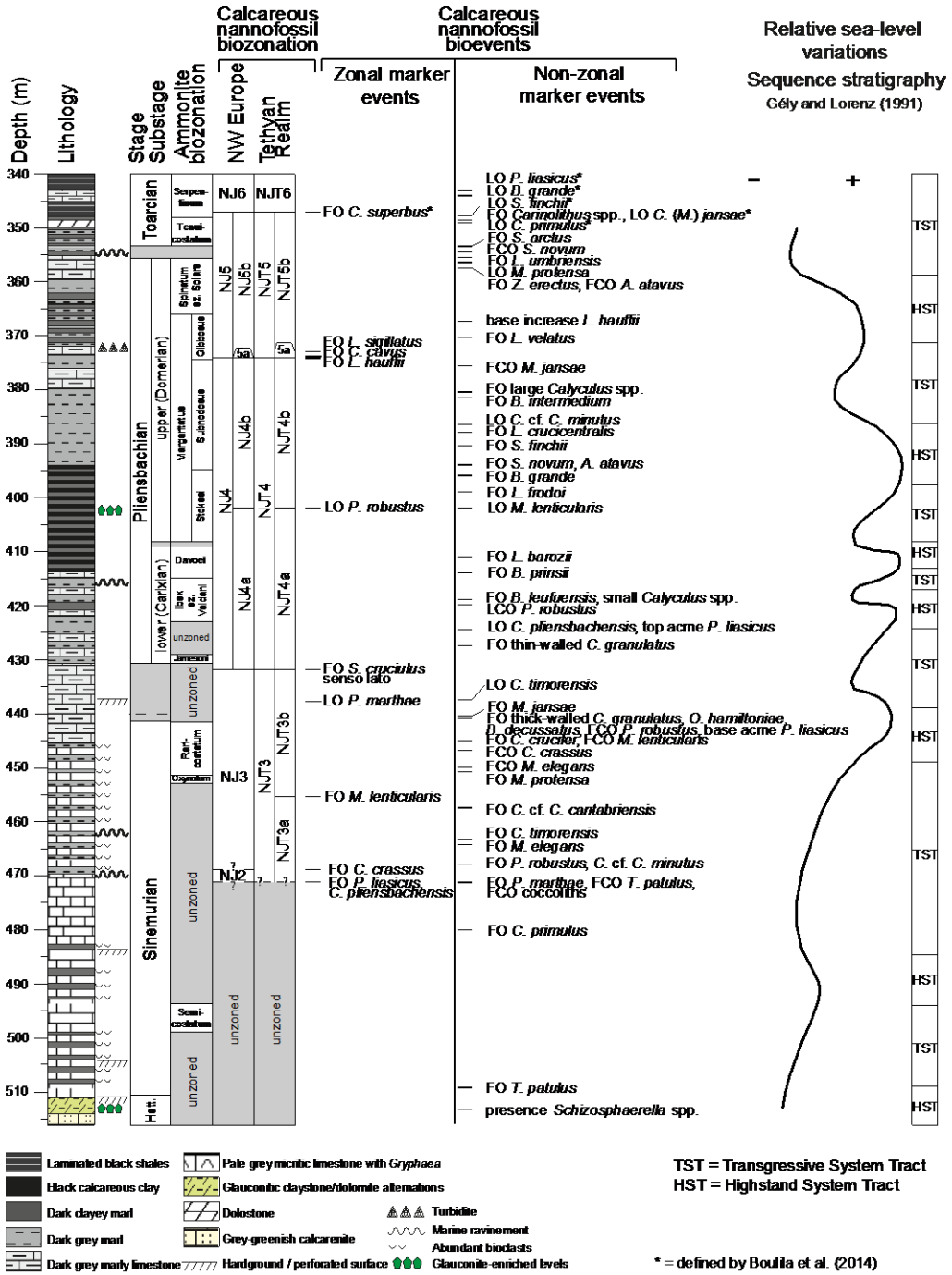

Figure 4: Calcareous nannofossil biostratigraphy of the Sancerre-Couy core. The relative sea-level curve and the sequence stratigraphic interpretation are from Gély and Lorenz (1991).

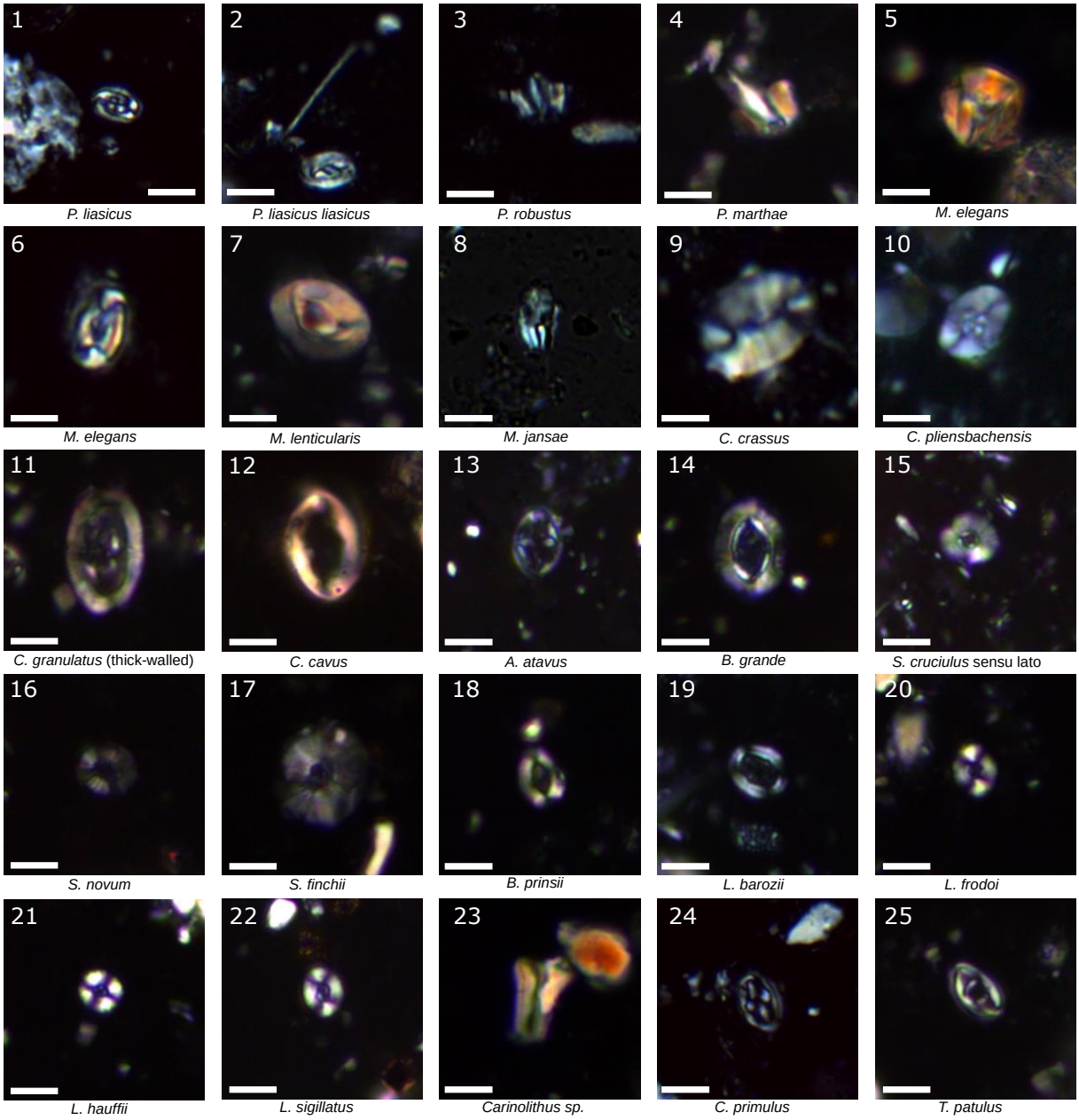

Figure 5: Main coccolith species of Sancerre-Couy. The scale bar is 5 µm long. Additional explanations including the age interval of illustrated specimens can be found in Appendix F.

Important species are illustrated in Figure 5, more specimens and other species are illustrated in the supplementary Figures S1, S2, S3 and S4 of Appendix F. with information regarding sample depth and age.

4.4. Organic carbon isotope fluctuations of the Sancerre-Couy core

Organic carbon isotope values of the Sancerre-Couy core reach from –30.8 ‰ to –24.5 ‰ (Fig. 5; Appendix G) with an average of –26.7 ‰. The lowermost ca. 10 m are characterized by large-scale fluctuations within calcarenite and glauconitic claystone and account for a sharp and short-lived positive excursion with values up to –25.0 ‰. The following ca. 40 m are characterized by a slight positive trend interrupted by a marked, small negative excursion around 497 m. Values fluctuate around a mean of –25.5 ‰ from ca. 470 to ca. 458m. Two sharp negative excursions separated by a small positive rebound constitute a well-marked 2 ‰ negative excursion spanning the Oxynotum AZ and the base of the Raricostatum AZ between 456.00 and 449.00 m. A large, stepwise negative trend is observed between 446 and 440 m where the most negative values of the entire studied section reach a mean of –30.8 ‰. This trend is followed by a stepwise increase up to 420.00 m with a return to values of ca. –25 ‰. Overall, this very

large, ca. 5 ‰ negative excursion spans the Raricostatum to the Ibex AZs. A 2.0 ‰ negative excursion composed of two main negative peaks and a short-lived rebound characterizes the 413-404 m interval, across the transition between the Davoei AZ and the Stokesi ASz. In contrast, the 404-396 m interval is characterized by a positive excursion reaching values up to –26 ‰ within the Stokesi ASz. Most of the Subnodosus ASz is characterized by a complex negative excursion composed of three distinct negative peaks and two small positive rebounds between 396and 382 m. This is followed by a positive event spanning the transition between the Subnodosus and Gibbosus ASzs at 382-370 m, which is characterized at its base by an extremely sharp 4.5 ‰ increase in δ13Corg. The interval between ca. 370 and 354 m spanning the upper half of the Gibbosus ASz and the entire Spinatum AZ is characterized by a negative excursion with mostly steady values around a mean of –27.5 ‰, interrupted by a short-lived positive excursion at ca. 365 m. The Pliensbachian–Toarcian transition is characterized by a positive excursion with values around –25 ‰, followed by the very sharp and pronounced 5 ‰ drop that characterizes the onset of the well-documented lower Toarcian negative carbon isotope excursion marking the Jenkyns Event (Fig. 5; Hesselbo et al., 2000, 2007; Hermoso et al., 2009; Müller et al., 2016).

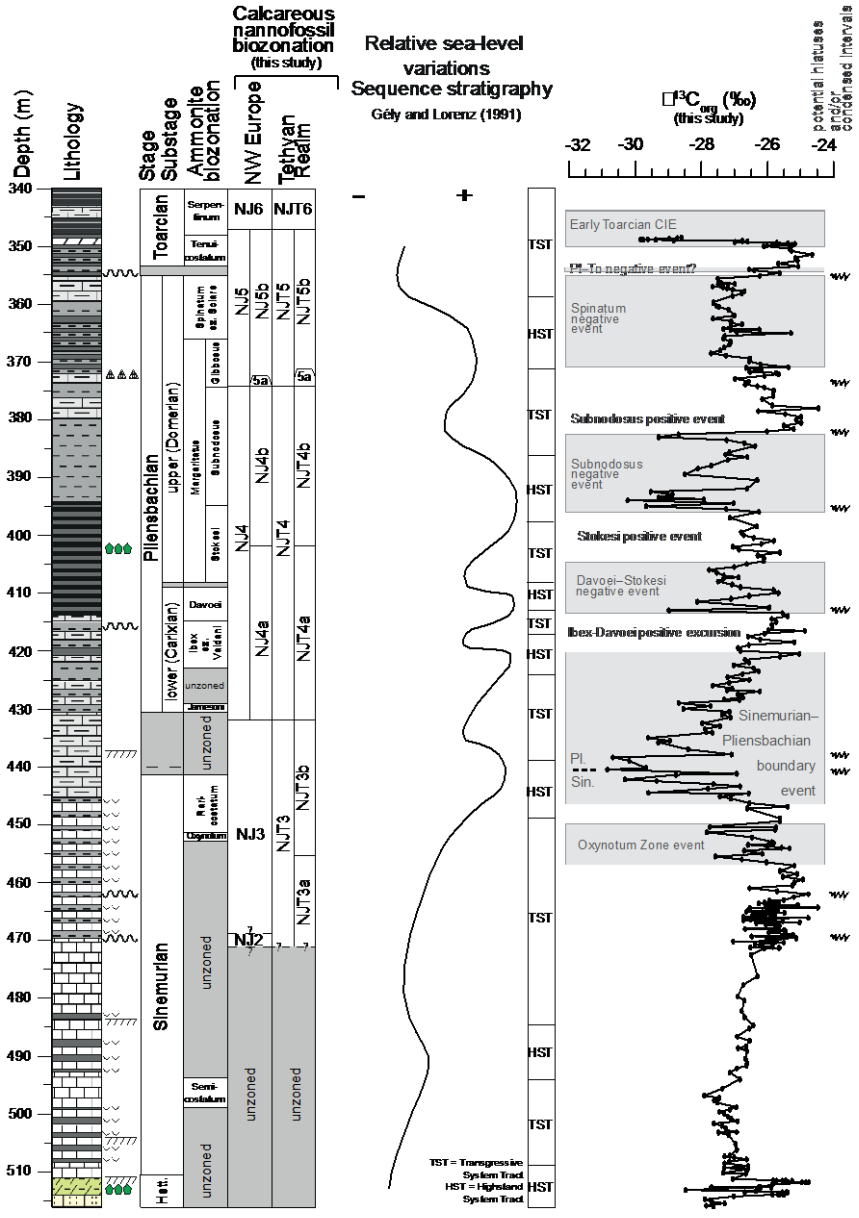

Figure 6: Organic carbon isotope fluctuations in the Sancerre-Couy core and putative gaps and/or condensed intervals as discussed in the text (Section 5.4) compared to the lithology, relative sea-level fluctuations and sequence stratigraphy. See Figure 2 for lithology legend. Relative sea-level curve and sequence stratigraphy after Gély and Lorenz (1991).

This is the author-formatted version of Peti et al., 2017, Palaeogeography, Palaeoclimatology, Palaeoecology 468, 142-161, http://dx.doi.org/10.1016/j.palaeo.2016.12.004

5. Discussion

5.1. Reliability of calcareous nannofossil bioevents

Numerous bioevents have been recorded in the Sancerre-Couy core. However, many species show inconsistent, sporadic occurrences that strongly affect the reliability of these bioevents (Table 1). For the first time, an evaluation of the reliability of all recorded Lower Jurassic bioevents is attempted in this study for the Paris Basin. It should be noted, however, that the evaluation of the reliability of bioevents is applicable only for the present core, and not at the regional or global scale. These results should be compared to other such records within the same basin, then to other Tethyan records.

Three distinct categories of reliability have been considered: dubious, reliable and robust (Table 1). If the species shows a continuous, consistent record after the FO, or preceding the LO, the biohorizon is considered to be robust. If a limited number of sporadic occurrences are recorded over a short, restricted interval immediately following the FO, or preceding the LO, the biohorizon is considered to be reliable. If the species is recorded discontinuously, following the FO, or preceding the LO, the biohorizon is considered to be dubious. By definition, FCOs and LCOs are considered to be robust bioevents as they mark the onset and end of a consistent record, respectively.

The FO of T. patulus, though considered here as dubious, may be close to the evolutionary first appearance datum of the species as it is recorded here just above the Hettangian/Sinemurian boundary, i.e. slightly earlier than its FO at the base of the Semicostatum AZ in the Cardigan Bay Basin (Bown, 1987). In contrast, the FO of C. primulus well above the Semicostatum AZ is here recorded much later than in the Mochras core where it first occurs within the Bucklandi AZ. The coincident FOs of P. liasicus and P. marthae are recorded in the upper half of the Sinemurian, well above Semicostatum, whereas they are found earlier, at the base of Semicostatum in the Cardigan Bay Basin (Bown, 1987). It is likely that the FO of C. primulus as well as the coincident FOs of P. liasicus, C. pliensbachensis and P. marthae can only be considered here as local events as they coincide with a significant rise in the absolute abundance of coccoliths which ismost probably related to a relative sea-level rise (Table 1; Fig. 4). These bioevents mark the establishment of favourable, pelagic conditions in the Paris Basin allowing coccolithophorids to thrive.

The evaluation of the robustness of bioevents has direct consequences for the reliability of applied standard biozonations at Sancerre-Couy. None of the bioevents used in the standard zonations of the upper Sinemurian to lower Pliensbachian can actually be considered as robust in this work. All marker species show inconsistent records following their FOs or preceding their LOs. In some cases, this inconsistency is quite dramatic. For instance, the FO of C. crassus is followed by isolated, single occurrences until the top of the Raricostatum AZ, i.e., 22 m above its FO (Fig. 3). Preservational issues can be excluded since C. crassus is a solution-resistant murolith coccolith (Bown, 1987; Mattioli and Erba, 1999). However, it is often subject to overgrowth resulting in difficulties of identification (Bown, 1987; Mattioli and Erba, 1999). Bown and Cooper (1998) pointed out that intermediate forms between C. crassus and its ancestor, probably C. pliensbachensis or C. timorensis, exist and this may account for discrepant FOs of C. crassus. It is suggested here that the inconsistent record immediately following its FO is also largely responsible for this discrepancy.

The LO of P. robustus placed in the Stokesi ASz is preceded by scattered single to rare occurrences (Fig. 3). Hence, this taxon can not be considered as a robust stratigraphic marker in our record. Conversely, the results of this study show that a number of bioevents not considered in standard biozonations appear as robust. Besides the FCOs and LCOs of numerous taxa proposed here as additional bioevents, a few species show very well-marked, consistent FOs and/or LOs. For instance, the FO of M. protensa is a robust bioevent of the Raricostatum AZ (Fig. 3). The LO of P. marthae constitutes a robust bioevent of the unzoned interval just below the Jamesoni AZ (Fig. 3). The LO of C. pliensbachensis is a robust bioevent in the unzoned interval just below the Ibex AZ (Fig. 3). The poor reliability of many bioevents in the upper Sinemurian is clearly linked to the lesser abundance of coccoliths due to shallower conditions (Gely and Lorenz, 1991). However, it is noticeable that even after the major rise in abundance of the coccoliths accompanying the transgression at the Sinemurian–Pliensbachian boundary (Fig. 4), many bioevents remain dubious in the lower Pliensbachian. In the upper Pliensbachian, the reliability of bioevents is generally better. Although it is considered as a secondary event, the LO of M. lenticularis appears in our record as a more robust bioevent for marking the base of the NJ4b/NJT4b Zone than the zonal standard LO of P. robustus (Figs. 3, 4). A number of successive, robust FOs are recorded within the NJ4b/NJT4b Subzone that may be used to refine and improve the stratigraphy of this subzone such as the FOs of L. frodoi, B. grande, S. novum, S. finchii, L.

crucicentralis and B. intermedium (Fig. 4; Table 1). The successive FOs of L. hauffii, C. cavus and L. sigillatus used in standard zonations (NJ5a and NJT5a) of the upper Pliensbachian are robust at Sancerre-Couy. The FOs of S. arctus and Carinolithus spp. also constitute robust bioevents of the lower Toarcian Tenuicostatum AZ, followed by consistent occurrences as shown in Clémence et al. (2015). Within the NJ5b/NJT5b Subzone, the FO of L. umbriensis defines a reliable additional bioevent (Fig. 4; Table 1). All recorded FCOs and LCOs of the Sancerre-Couy record are not discussed further here but they represent new bioevents that merit proper testing in other cores/ sections of the Paris Basin and in other oceanic realms.

5.2. Comparison to other areas

Comparison of calcareous nannofossil occurrences and biozones between the different domains of the peri-tethyan realm is not a straightforward task as these domains have distinct ammonite zonations but also because the concepts applied to ammonite zones are not always strictly based on the presence of index taxa and may be defined by a particular assemblage of species (see for instance the definition of the base of the Polymorphum AZ at Peniche, Rocha et al., 2016). These issues may be partly responsible for the apparent diachronism of nannofossil taxa between distinct oceanic basins of the peritethyan realm.

5.2.1. Main bioevents defining calcareous nannofossil zones

Bown and Copper (1998) place the base of the NJ2 Zone in the uppermost Hettangian (Fig. 7a), much earlier than recorded in the Sancerre-Couy core (Fig. 7b). This discrepancy results from the delayed FO of P. liasicus in the Paris Basin that we relate to a major sea-level rise (see sections 4.3, 5.1). The assigned base of NJ2 and NJT3 coincide in our record. However, they do not correspond to the base of the respective zones because we record the FO of the corresponding stratigraphic markers at the same time as the significant rise in coccolith abundance which marks a local event linked to the relative sea-level rise (Fig. 4, section 5.1). Consequently, we cannot place the base of these zones correctly at Sancerre-Couy (Fig. 7b).

The standard zonation from Bown and Cooper (1998) was mainly based on investigations from the UK (SW England, Wales) by Bown (1987). The NJ2b and NJ3 Zones (originally JL2b and JL3) have been originally defined by results obtained on the Mochras core. Van de Schootbrugge et al. (2005) describe the palaeogeographic position of this core as close to the depositional centre of the Cardigan Bay Basin under the continuous influence of subsidence. The Sinemurian to Toarcian carbonate facies of the Mochras core thus logically represent deeper depositional environments as compared to those of the Sancerre-Couy core. The discrepancy in the timing of the bioevents defining the Hettangian to mid-Sinemurian calcareous nannofossil zones NJ1-NJ2 between the Cardigan Bay Basin and this study supports our interpretation of a major influence of the relative sea-level rise on the sudden appearance and subsequent consistent occurrence of coccolithophorids in the upper Sinemurian of the Paris Basin. The proposed subdivision of Bown and Cooper (1998) into the NJ2a Parhabdolithus marthae Subzone and the NJ2b Mitrolithus elegans Subzone based on the LO of P. marthae cannot be achieved here as the LO of P. marthae is recorded much much above the FO of C. crassus (Fig. 4).

The base of the NJ3 Zone is placed in the lower part of the Oxynotum AZ based on the FO of C. crassus (Bown and Cooper, 1998; Fig. 7a). Only the top of the Oxynotum AZ could be identified in the Sancerre-Couy core and it remains unclear whether or not the base of NJ3 as identified here would correlate to the Oxynotum AZ (Fig. 7b). Considering the average thickness of ammonite zones in the core and the distance of this stratigraphic level to the top of the Oxynotum AZ, this level may project to a similar level in the Paris Basin or to a slightly younger ammonite zone such as the Obtusum AZ (Fig. 7a). The base of NJT3 as defined by the FO of C. pliensbachensis appears time-transgressive between (1) the Mediterranean area where it is recorded at the top of the Bucklandi AZ (Fig. 7a), slightly below the base of the Semicostatum AZ (Fig. 7a) and (2) the Paris Basin (only 2.3 m below the base of NJ3, projecting well above the Semicostatum AZ; Fig. 4). The base of the NJT3b Subzone is considered more or less coincident to the base of the Raricostatum AZ in the standard zonation (Fig. 7a). At Sancerre-Couy, the base of NJT3b is placed slightly lower, most probably projecting within the upper part of the Oxynotum AZ (Figs. 4, 7b). The dubiousness of the FO of M. lenticularis at Sancerre-Couy may account for this discrepancy. It is possible that this species shows similar inconsistent very rare to single occurrences at the base of its range in other oceanic domains, thus creating a great uncertainty in the exact position of this bioevent at a wide geographic scale. It is possible that the FCO of M. lenticularis in the Paris Basin (within the Raricostatum AZ) actually correlates better to its FO in the Lusitanian Basin (Fig. 7; Mattioli et al., 2013).

This is the author-formatted version of Peti et al., 2017, Palaeogeography, Palaeoclimatology, Palaeoecology 468, 142-161, http://dx.doi.org/10.1016/j.palaeo.2016.12.004

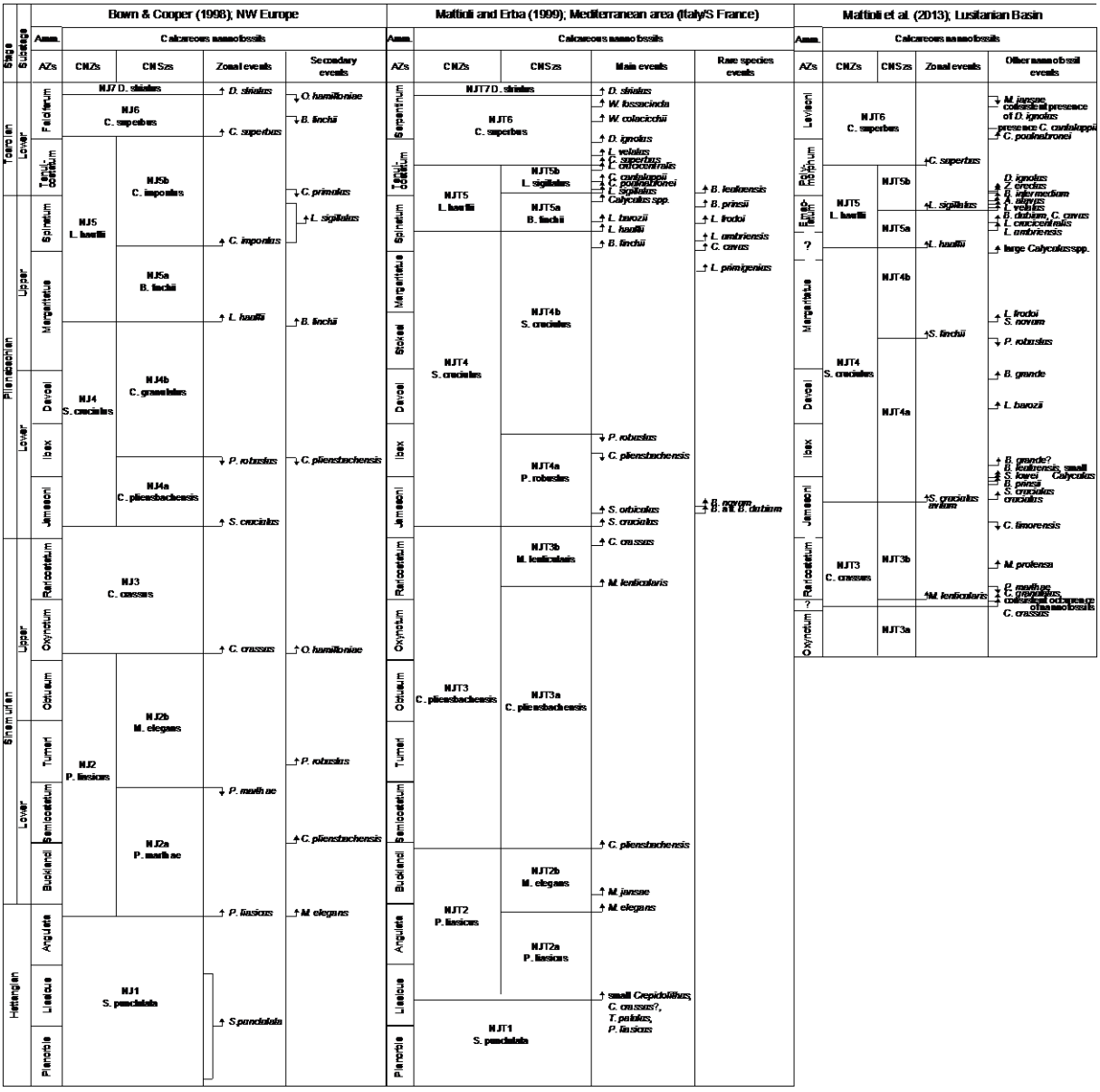

This is the author-formatted version of Peti et al., 2017, Palaeogeography, Palaeoclimatology, Palaeoecology 468, 142-161, http://dx.doi.org/10.1016/j.palaeo.2016.12.004

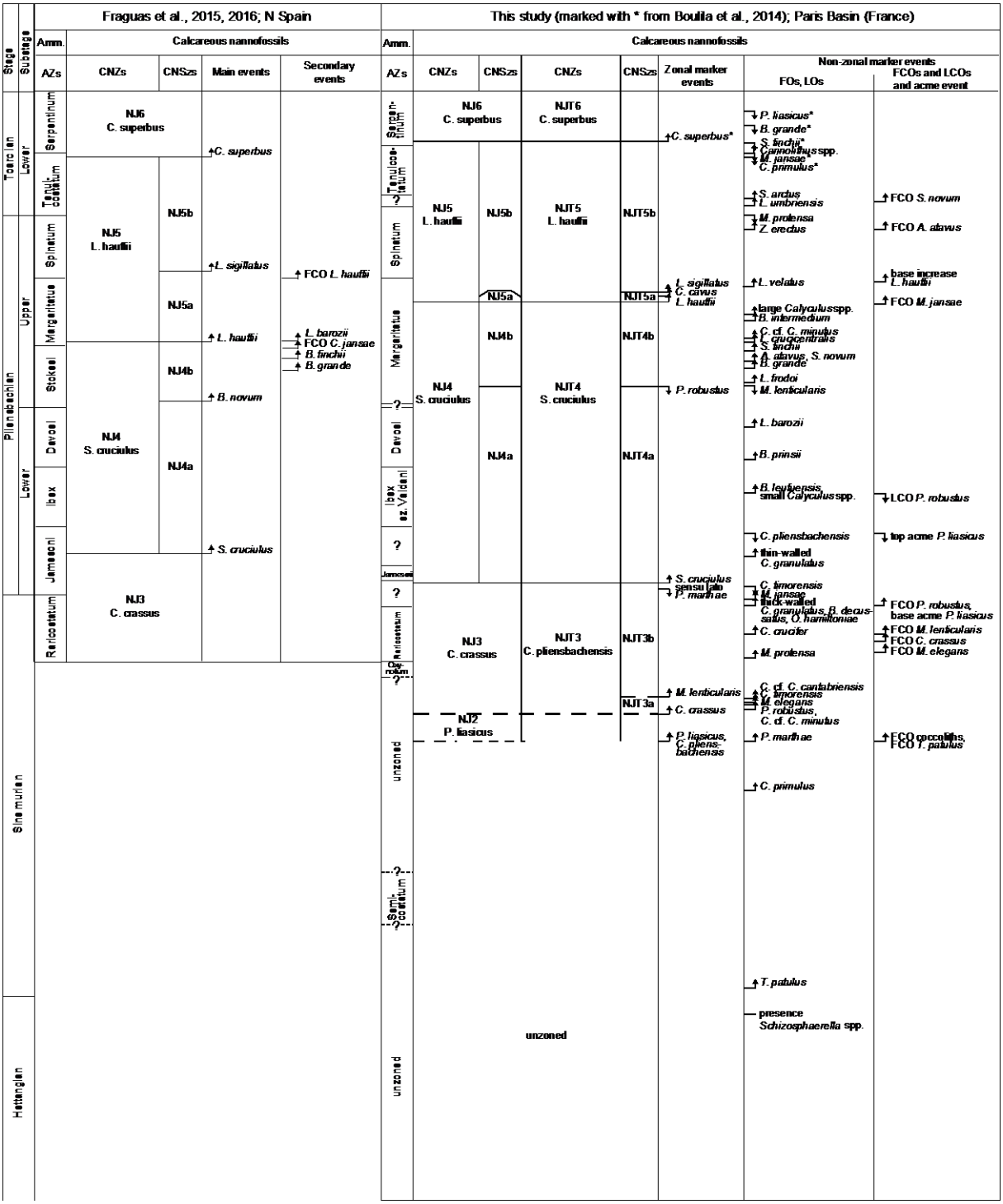

Figure 7: Comparison of the calcareous nannofossil zonation and main calcareous nannofossil bioevents of this study (Paris Basin, France) with that of NW Europe (Bown and Cooper, 1998), Italy/S France (Mattioli and Erba, 1999), Lusitanian Basin (Portugal, Mattioli et al., 2013) and N Spain (Fraguas et al., 2016) correlated to their respective ammonite zonations. Amm.: Ammonites; AZs: Ammonite Zones; CNZs: Calcareous nannofossil zones; CNSzs: Calcareous nannofossil subzones. Dashed lines represent uncertain positions of zone boundaries.

The base of the NJ4/NJT4 zones appears consistently placed in the Jamesoni AZ throughout the different oceanic domains (Bown and Cooper, 1998; Mattioli and Erba, 1999; Mattioli et al., 2013; Fig. 7a) as it is just slightly below the identified Jamesoni AZ in the unzoned interval of our record (Figs. 4, 7b). Its position lies above the Sinemurian–Pliensbachian boundary as identified at 440m by Lorenz et al. (1987) and further confirmed by carbon isotope stratigraphy (see section 5.3). These observations suggest a simultaneous first appearance of *S. cruciulus* in the peri-tethyan realm, which also represents the important evolutionary emergence of placoliths (Mattioli et al., 2013; Plancq et al., 2016).

The bases of the NJ4b/NJT4b subzones are defined in NW Europe (mostly England) and in the Mediterranean area (Italy and South France) by the LO of P. robustus within the lower part of the Ibex AZ (Fig. 7a; Bown and Cooper, 1998; Mattioli and Erba, 1999). The latter authors proposed the LO of C. pliensbachensis as a secondary marker for the base of this zone (Fig. 7a). In our record, the LO of C. pliensbachensis is a robust bioevent, recorded in the unzoned interval right below the base of the Ibex AZ (Fig. 4), and this bioevent correlates well with its LO as recorded in other oceanic domains. In the Lusitanian Basin, the LO of P. robustus is recorded much higher, namely in the lower Margaritatus AZ (Mattioli et al., 2013, Fig. 7a) correlating well to the higher position of the LO of P. robustus in the Paris Basin (Stokesi ASz, Fig. 4, 7b). Fraguas et al. (2015, 2016) do not locate the LOs of P. robustus or C. pliensbachensis on their synthetic figure, but according to their data and despite generally rather low abundances of these species, their LOs fall respectively within the Davoei and Ibex AZs (Santontis section), within the Ibex AZ and uppermost Jamesoni AZ (Tudanca section) and within the Ibex AZ (Camino section). i.e. much earlier than in the Lusitanian and Paris Basin but correlating better to NW Europe (Bown and Cooper, 1998) and the Mediterranean realm (Mattioli and Erba, 1999). Interestingly the LCO of P. robustus is recorded within the Ibex AZ at Sancerre-Couy, just slightly above the LO of C. pliensbachensis (Fig. 4). Hence, the LCO of P. robustus and the LO of C. pliensbachensis in the Paris Basin likely correlate to the LO of P. robustus in NW Europe (Bown and Cooper, 1998) and in the Mediterranean area (Mattioli and Erba, 1999, Fig. 7). Due to these discrepancies and probably due to the paucity of P. robustus in the Cantabrian range, Fraguas et al. (2015) propose the use of the FO of B. novum (synonymous to S. novum of some authors) to define the base of the NJ4b Subzone in N. Spain. The latter bioevent is recorded at the base of the Stokesi ASz in N. Spain, at the base of Subnodosus ASz in the Paris Basin, in the top of the Jamesoni AZ in the Mediterranean area and in the top upper third of the Margaritatus AZ in the Lusitanian basin (Fig. 7). Therefore this bioevent appears strongly diachronous across distinct oceanic realms and is probably not the best reliable marker for the base of NJ4b when P. robustus cannot be used. Note that Mattioli et al. (2013) used the FO of S. finchii to define the base of NJT4b in the Lusitanian Basin (Fig. 7A).

Bown and Cooper (1998) define the base of the NJ5 Zone in NW Europe by the FO of L. hauffii in the middle part of the Margaritatus AZ (Fig. 7a). In the Mediterranean area (Mattioli and Erba, 1999), this level projects to the basal part of the Spinatum AZ whereas it falls in-between the Margaritatus and the Emaciatum AZs in the Lusitanian Basin (Mattioli et al., 2013), and into the basal part of the Margaritatus AZ in Cantabrian range (Fraguas et al., 2015, 2016; Fig. 7). This important discrepancy for the base of NJ5/NJT5 is possibly linked to a diachronous FO of L. hauffii according to Fraguas et al. (2015). In the Paris Basin, the FO of L. hauffii is recorded within the lowermost part of the Gibbosus ASz (Fig. 4) and therefore correlates slightly better with its stratigraphic level in the Mediterranean area and in the Lusitanian Basin (Fig. 7a).

The base of the NJ5b Subzone was originally defined by the FO of C. impontus (synonymous of C. cavus) in the lowermost part of the Spinatum AZ (Fig. 7a). In our record, the FO of C. cavus occurs immediately above the FO of L. hauffii, in the topmost part of the Margaritatus AZ (Figs. 4, 7b), consequently accounting for only a slight discrepancy with respect to the NW European scheme. Mattioli and Erba (1999) consider the FO of L. sigillatus to define the base of the NJT5b Subzone in the lowermost Toarcian (Tenuicostatum AZ) despite mentioning sporadic occurrences of this taxon in the uppermost Pliensbachian of a few studied sections (Fig. 7a). Mattioli et al. (2013) place this bioevent within the Emaciatum AZ in the Lusitanian Basin (Fig. 7a) and Fraguas et al. (2015) use the FO of L. sigillatus at the base of the Spinatum AZ to define the base of the NJ5b Subzone in the Cantabrian range (Fig. 7b). The position of the FO of L. sigillatus in the topmost part of the Margaritatus AZ in the Sancerre-Couy core thus marks the lowermost FO of this species compared to any other records (Fig. 7b). It is unclear whether or not this apparent diachronism of the FO of L. sigillatus across distinct oceanic realms is due to the application of different ammonite zonation schemes or not. Fraguas et al. (2015) mention the possibilty that L. sigillatus first originated in the northern areas and spread later into the southern areas of the peritethyan realm. This hypothesis is supported by the presence of ammonite fauna with a clear boreal affinity but also of Tethyan assemblages at different stratigraphical levels, which led Fraguas et al. (2015) to suggest that the Cantabrian range was a potential connection area between NW Europe (Boreal Realm) and the Tethyan Realm.

The base of the NJ6/NJT6 zones, as defined by the FO of C. superbus, appears to project slightly lower in the southern realms (mid- to upper part of the Tenuicostatum and Polymorphum AZs; Fig. 7; Mattioli and Erba, 1999, Mattioli et al., 2013, Fraguas et al., 2015, 2016) compared to NW Europe (basal part of the Serpentinum AZ; Fig.

7a; Bown and Cooper, 1998) and the Paris Basin (basal part of the Serpentinum AZ at Sancerre-Couy; Fig. 7b). Mattioli and Erba (1999) mention the rarity of C. superbus in the lowermost Toarcian as a possible cause for such discrepancies.

5.2.2. Secondary bioevents

The FCO of the overall coccolith assemblage during the Sinemurian relative sea-level rise correlates relatively well with the same horizon in the Lusitanian Basin (Fig. 7a). All the bioevents of the mid-Sinemurian interval (ca. 480-455 m) are dubious (Fig. 4; Table 1), and they are not calibrated to the ammonite standard zonation. Therefore, comparison to other regions is difficult.

The acme event of P. liasicus offers two new robust secondary bioevents at its base and top, in unzoned intervals across the Sinemurian–Pliensbachian boundary. The FO of C. granulatus is recorded slightly lower at the top of the Oxynotum AZ in the Lusitanian Basin (Fig. 7a) compared to the top of the Raricostatum AZ in the Paris Basin (Fig. 7b). It is worth mentioning that this species bears two distinct morphotypes, one with a thick wall occurring lower in the top of the Raricostatum AZ, and one with a thin wall, which first occurs higher up in the unzoned interval below the Ibex AZ (Fig. 4).

The LO of C. timorensis within the unzoned interval right below the base of the Jamesoni AZ (Fig. 7b) correlates well to results of the Lusitanian Basin where it is recorded in the base of the Jamesoni AZ (Fig. 7a). This LO serves as a reliable additional bioevent with high potential to be incorporated in future refined zonation schemes.

Similarly to Mattioli et al. (2013), we differentiate between small and large Calyculus spp. (Plate 4, 24-27). The FO of Calyculus spp. occurs simultaneously in the Lusitanian Basin (as small specimens, base of the Ibex AZ; Fig. 7a; Mattioli et al., 2013), in the Cantabrian Range (no differentiation between small and large specimens, within the Ibex AZ; Fig. 7b; Fraguas et al., 2015) and in the Paris Basin (as small specimens, within the Ibex AZ; Fig. 7b; this study). The FO of small Calyculus spp. also coincides exactly with the FO of B. leufuensis in both the Lusitanian and Paris Basin (Fig. 7). In the record of Italy and South France, both events occur extremely close to each other even though this double-event is always recorded at different times from one section to another (Mattioli and Erba, 1999; Fig. 7a). Moreover, large Calyculus spp. first occur nearly concomitantly in the Lusitanian Basin and the Paris Basin in the mid- to upper part of the Margaritatus AZ, thus providing two potential additional supra-regional bioevents. The emergence of large Calyculus spp. appears to have occurred at the same time in the different domains, suggesting a potential link to a common environmental cause. It is also noteworthy that small Calyculus spp. tend to disappear when large forms appear.

Large discrepancies remain with respect to the FO of B. prinsii. In the Lusitanian Basin (Mattioli et al., 2013), this species first occurs in the Jamesoni AZ followed by its FO in the Davoei AZ in northern Spain (Fraguas et al., 2015) and in the Paris Basin (this study), within the Spinatum AZ in Italy and South France (Fig. 7, Mattioli and Erba, 1999), and finally at the Pliensbachian–Toarcian boundary in Wales, UK (Bown, 1987). These significant discrepancies may point towards a time-transgressive colonization of B. prinsii roughly from south to north of the peri-tethyan realm.

The FO of L. barozii in the Paris Basin correlates well to the Lusitanian Basin within the Davoei AZ. However, in Italy and South France and northern Spain, L. barozii first occurs in the Spinatum and Margaritatus AZs, respectively (Fig. 7). Both studies record a concomitant FO of L. barozii and L. hauffii. Reasons for these inconsistencies may be connected to taxonomic difficulties in the identification of the different Lotharingius species, to preservational issues, or, once again, to time-transgressive colonization of different oceanic domains as supported by Fraguas et al. (2015) for other species of the genus Lotharingius.

The LO of M. lenticularis is proposed here as an additional marker for the base of the NJ4b/NJT4b subzones due to its concomitant occurrence with the LO of P. robustus and to its robustness (Fig. 3; Table 1). Data of Fraguas et al. (2015) suggest a LO of this species in the Margaritatus AZ as well but it is not consistently recorded in all investigated sections.

The FO of L. frodoi correlates well between the Paris Basin and the Lusitanian Basin in the Margaritatus AZ (Fig. 7). It may be considered as a potential bioevent or refinement of the NJT4b Subzone.

The FO of B. grande in the Stokesi ASz correlates well to its position in the Stokesi AZ (considered to be the lowermost ASz of the Margaritatus AZ in the present study) in the Cantabrian Range (Fig. 7b). The first appearance of B. grande is recorded earlier in the Lusitanian Basin (within the Davoei AZ; Fig. 7a). According to Mattioli and Erba (1999), this species is considered a characteristic constituent of Toarcian assemblages in the Tethyan Realm. B. grande thus appears to have a Tethyan affinity and an emergence in the southern peri-tethyan

realm, followed by a delayed colonization of northern areas is hypothesised here.

The FO of S. finchii is consistently recorded within the Margaritatus AZ. This bioevent is promising for supra-regional correlation as already suggested by Mattioli et al. (2013).

Fraguas et al. (2015) proposed the use of a new useful bioevent, the FCO of M. jansae which is also recorded in our study (Fig. 7b). In terms of ammonite zonation however, this event is located lower in the Cantabrian Range (top of the Stokesi ASz; Fig. 7b) than in the Paris Basin (top of the Subnodosus ASz; Fig. 7b).

The FO of L. velatus within the Gibbosus ASz in the Paris Basin does not correlate very well with its FO within the Emaciatum AZ in the Lusitanian Basin (Fig. 7, Mattioli et al., 2013). However, as precised in the recent study of Rocha et al. (2016), L. velatus is now split in two distinct morphotypes, L. velatus sensu stricto and L. aff. L. velatus whose FO are distinct. Lotharingius aff. L. velatus which has a thinner rim than L. velatus first occurs in Emaciatum AZ whereas L. velatus sensu stricto first occurs in Polymorphum at Peniche (Rocha et al., 2016). In our study, we did not make a strict distinction between the two different forms although both of them are illustrated in Appendix F.

Fraguas et al. (2015) define the FCO of L. hauffii in the lowermost part of the Spinatum AZ which corresponds to our 'base increase L. hauffii' (upper part of the Margaritatus AZ). In both cases, this bioevent lies close to the FO of L. sigillatus. The marked increase in the abundance of the species may be considered as another additional marker for the base of the NJT5b Subzone.

The FO of L. umbriensis is recorded concomitantly within the Spinatum AZ in the Lusitanian Basin, in Italy and South France and in the Paris Basin (Fig. 7). The newly defined FCO of A. atavus in the top of the Spinatum AZ is more reliable than its FO in the Paris Basin and correlates relatively well to its FO in the Lusitanian Basin (Fig. 7). The FO of Z. erectus in the immediate vicinity of the Pliensbachian–Toarcian boundary correlates well between the Lusitanian and Paris Basins (Fig. 7).

Similar high-resolution nannofossil biostratigraphic records are needed for this interval in order to test all the new potential markers considered here. However, our study shows that a large number of additional bioevents could be considered in the Lower Jurassic, allowing for a significant improvement of standard biozonations.

5.3. A high-resolution organic carbon isotope curve for the Sinemurian–Pliensbachian of the NW Tethys

The new high-resolution record of organic carbon isotopes of the Sancerre-Couy core allows for the definition of numerous negative and positive carbon isotope excursions (CIE; Fig. 6), some of which have already been identified in other records spanning the same time interval.

The lowermost positive CIE right below the Hettangian–Sinemurian boundary is dubious as it occurs within very shallow glauconitic and dolomitic facies. It may represent a local event only, due to the potential mixing of various sources of continental and marine organic matter, whose average values differ considerably (Suan et al., 2015), as well as to potential diagenetic alteration of the organic matter during dolomitization. Hettangian–Sinemurian boundary records have been generated from different sections, of which successions in the USA point to a positive CIE below the Hettangian–Sinemurian boundary, whereas published European records do not show a clear isotopic shift (van de Schootbrugge et al,. 2008; Ruhl et al., 2010; Bartolini et al., 2012).

A small negative CIE is recorded within the Semicostatum AZ but its amplitude is rather small (ca. 1 ‰) as compared to other, more prominent features recorded higher up in the core. Therefore, we do not define here any significant event in most of the Sinemurian although some trends may potentially correlate to recent studies on organic matter in UK and North America (Jenkyns and Weedon, 2013; Porter et al., 2014). Significant organic carbon isotope events can be defined with more confidence in our record from the upper Sinemurian to the top of the Pliensbachian. The first well-marked 2 ‰ negative CIE spanning the Oxynotum AZ to base of the Raricostatum AZ at Sancerre-Couy has already been documented in the Cleveland Basin (van de Schootbrugge et al., 2005), where it is similarly expressed by an amplitude of ca. 2 ‰ in bulk carbonate δ13C (δ13Ccarb), in bulk organic matter (δ13Corg) as well as selected palynomorphs and belemnite calcite (δ13Cbelemnite). This excursion is expressed by two negative peaks surrounding a positive rebound (Riding et al., 2013) and this is similar in our record (Fig. 6). The timing of this excursion appears to match relatively well that documented by Riding et al. (2013) across the upper part of the Turneri AZ to the base of the Raricostatum AZ. In the Sancerre-Couy record, this excursion referred here as the "Oxynotum Zone event" represents a precursor negative CIE of the larger and longer-lasting negative CIE of the Sinemurian–Pliensbachian boundary event

(SPBE; Fig. 6). This excursion does not appear clearly in the δ13Cbelemnite in the recent review by Gomez et al. (2016). The SPBE, however, is very well-expressed at Sancerre-Couy by a large amplitude ~5 ‰ excursion (Fig. 6). In the Cleveland (UK) and Lusitanian (Portugal) Basins, and in the Trento Platform (Italy), the excursion is expressed in the calcite of marine fossils, in bulk carbonate, in bulk organics and/or in fossil wood (Korte and Hesselbo, 2011; Duarte et al., 2014; Franceschi et al., 2014). The position of the onset and top of the excursion may be subject to discussion. In the three latter studies, the onset of the SPBE is very near the base of the Jamesoni AZ, where the bulk of the drop in carbon isotopes occurs, but the review by Gomez et al. (2016) tend to place the onset of the SPBE at the base of the Aplanatum ASz of the Raricostatum AZ. Either way, the most positive values preceding this decrease are situated within the Raricostatum AZ in the UK and in northern Spain. This is similar to the way we define the onset of the excursion at Sancerre-Couy (Fig. 6). The most negative values of this excursion are reached exactly at the Sinemurian–Pliensbachian boundary (Korte and Hesselbo, 2011; Gomez et al., 2016) corresponding well to our record where they are situated within the unzoned interval between the Raricostatum and Jamesoni AZs. Consequently, the stratigraphy at Sancerre-Couy may be refined here by carbon isotope stratigraphy with the most negative values at 440.50 m indicating the position of the Sinemurian–Pliensbachian boundary (Fig. 6). This position agrees well with the position of the boundary as originally given at 440 m by Lorenz et al. (1987).

In this study, we position the top of the SPBE at the end of a full 5 ‰ recovery from the negative CIE, where values reach another local maximum. This positionconstitutes the base of a positive CIE spanning the transition between the Ibex and Davoei AZs, defined as the Ibex–Davoei positive CIE in δ13Cbelemnite in Gomez et al. (2016), a name which is retained here (Fig. 6). A similar δ13C trend has been observed by Morettini et al. (2002) on bulk carbonates of central Italy and by Armendariz et al. (2012) in belemnite calcite from the Asturian Basin. Silva et al. (2011) record a positive δ13Ccarb excursion in the Davoei AZ of the Lusitanian Basin.

The upper Pliensbachian has been found to be mostly characterized by the long-lasting 'Late Pliensbachian positive CIE' (Gomez et al., 2016). In contrast, in the Sancerre-Couy core, bulk organic matter shows additional potential excursions. Immediately following the SPBE, we define here the Davoei–Stokesi negative event as a double excursion interrupted by a positive rebound with an amplitude of 2.0 ‰. A negative CIE around the Davoei AZ is also visible in δ13Ccarb and δ13Corg in the record of the Mochras core (van de Schootbrugge et al., 2005). Immediately above the latter excursion, the Stokesi positive event is defined exactly within the Stokesi ASz.

The Subnodosus negative event spans the uppermost part of the Stokesi ASz and the Subnodosus ASz. It is defined in this record as a triple negative peak interrupted by two positive rebounds with an amplitude of 4 ‰ (Fig. 6). The Subnodosus positive event is defined at its base by a sharp 4.5 ‰ increase and at its top by a 2 ‰ return to more negative values (Fig. 6). Although all the preceding events cannot be identified clearly in the Cleveland dataset of marine fossils and fossil wood, the Subnodosus event as defined here may be the expression of the pronounced, up to 60 ‰ positive CIE in fossil wood spanning the Subnodosus and Gibbosus ASzs, and called "Late Pliensbachian Event" by Korte and Hesselbo (2011). This name is not recommended here as numerous excursions appear to characterize the upper Pliensbachian and because this name was also used by Littler et al. (2010) to define a negative CIE in bulk organic matter which is characteristic of the Pl–To transition.

The remainder of the Pliensbachian is characterized here by the Spinatum negative event which has an amplitude of ca. 2 ‰ (Fig. 6) and spans the uppermost part of the Gibbosus ASz and the entire Spinatum AZ at Sancerre-Couy (which corresponds only to the Apyrenum ASz). The Spinatum negative event defined here is considered as part of the 'Late Pliensbachian positive CIE' in the δ13Cbelemnite of Gomez et al. (2016). However, the Spinatum negative event deserves to be clearly delineated as a distinctive negative trend which can also be observed in nearly every region and every carbon species in the Spinatum AZ (see figure 6 of Gomez et al., 2016 as well as Quesada et al., 2005; Veiga de Oliveira et al., 2006; Korte and Hesselbo, 2011; Martinez and Dera, 2015; Silva and Duarte, 2015).

The Pl-To negative event is defined in accordance to the studies of Littler et al. (2010) in Yorkshire, Suan et al. (2010) and Rocha et al. (2016) at the Peniche Global Boundary Stratotype Section and Point (GSSP) for the base of the Toarcian. It is a negative carbon isotope excursion present in all carbon species across the Pliensbachian–Toarcian boundary and at the base of the Toarcian. This event may be distinguished in the Sancerre-Couy core by a -1 ‰, small-amplitude negative event situated exactly at the Pl.-To transition. The poor expression of this event at Sancerre-Couy is likely

due to the important condensation of the Pl-To transition in the core as previously discussed. The early Toarcian CIE is marked by a sharp drop in δ13Corg in the upper Tenuicostatum AZ at Sancerre-Couy (Fig. 6).

5.4. Condensation and gaps in the Paris Basin record as demonstrated by integrated bio- and chemostratigraphy

Biostratigraphic results of ammonites and calcareous nannofossils, as well as the characteristic shape of many organic carbon isotope excursions argue for numerous condensation intervals and/or gaps throughout the Sinemurian–Pliensbachian time interval of the Sancerre-Couy core. This interpretation is in accordance with the finding of several distinct hardgrounds and marine ravinements in the core (Figs. 2, 6). A first major condensed interval is the glauconitic horizon across the Hettangian–Sinemurian transition associated with a much perturbed carbon isotope signal. A second major interval of condensation is suggested at 471.00 m in the large unzoned interval of the Sinemurian situated in-between the Semicostatum and Oxynotum AZs. There, the sudden FCO of coccoliths is accompanied by the coincident FO of no less than three distinct species of coccoliths. This major origination event also coincides with a major change of facies from homogeneous pale grey micritic limestone with Gryphaea to alternations of micritic limestones and bioclastic grey marls indicating deepening (Fig. 6). A marine ravinement is also noticed exactly at this facies transition, suggesting that this stratigraphic level corresponds to an important transgressive surface in contrast to the sequential model of Gély and Lorenz (1991) (Fig. 2). Nannofossil origination events appear more stepwise in the remaining of the Sinemurian. At the top of the Raricostatum AZ, a second major origination event of four distinct species is recorded at 440.80 m and coincides with a sudden increase in the abundance of the overall coccolith assemblage. This depth corresponds to a sharp and short-lived, positive 4.0 ‰ δ13Corg excursion 30 cm below the most negative values of the SPBE (Fig. 6). The coincidence of the two latter features may point to another condensation. At 437.70 m, a hardground is coincident with a second, very sharp, 4.0 ‰ positive CIE at 437.7 m (Fig. 6). Therefore, the entire interval spanning the Sinemurian–Pliensbachian boundary and corresponding to the most negative values of the SPBE beyond –29.0 ‰, is characterized by numerous condensed intervals. These results may indicate a major deepening and condensation of this interval associated with maximum flooding as proposed by Gély and Lorenz (1991) (Fig. 2). The lower–upper Pliensbachian transition appears as another potentially condensed interval as suggested by the FO of at least nine different ammonite species between 412.00 and 407.50 m (Appendix D). Condensation at 412.00 m is also strongly suggested by the sharpness of the drop in organic carbon isotopes which characterizes the base of the Davoei–Stokesi negative event (Fig. 6). The Subnodosus negative event is characterized at its base and at its top by very sharp shifts in carbon isotopes suggesting once again that this event is bounded by two condensed intervals at 396.00 and 382.00 m. The extreme thinness of nannofossil subzones NJ5a and NJT5a also suggest a major condensation at the base of the Gibbosus ASz. This is concordant with the supposed presence of an erosive, graded bed, interpreted as a turbidite at the top of NJT5a, which probably eroded a relatively large part of the first subzone of NJ5 (Fig. 2). This turbidite remains putative though, as this level could not be observed by us as it has been borrowed by previous workers who left a descriptive note in the core box. The Subnodosus positive event is interrupted by a small 1.3 ‰ negative excursion spanning the NJ5a/NJT5a subzones (Fig. 6). This negative excursion could be truncated here and may represent the biased expression of a negative event with a larger amplitude elsewhere. The absence of the Hawskerense ASz of the Spinatum AZ in the Sancerre-Couy core, together with the presence of a marine ravinement at 355.05 m, strongly argue for the uppermost Pliensbachian and Pl–To transition being characterized by an important hiatus. These observations are concordant with the sharpness of the increase in carbon isotope values which characterize the top of the Spinatum negative event as well as with the very poor expression of the Pl–To negative CIE across the Pl–To boundary transition. The Pl-To transition also corresponds to an important condensation in the Lusitanian Basin due to rapid transgression (discontinuity D1 in Pittet et al., 2014). Given a total duration of the Spinatum AZ of ca. 1.5 Myr (GTS2012), and assuming an equal duration for the Apyrenum and Hawskerense ASzs, it can be estimated here that the identified hiatus may span up to ca. 750 kyr of the uppermost Pliensbachian. Moreover, the Tenuicostatum AZ is mostly represented at Sancerre-Couy by its last Semicelatum ASz. Given the approximate duration of 1.05 Myr for the Tenuicostatum AZ (GTS2012), it can be grossly estimated that the Pl–To hiatus spans an additional 750 kyr of the base Toarcian and therefore accounts for a total duration of ca. 1.5 Myr across the Pliensbachian–Toarcian

boundary. The latter time span is a gross estimation for the duration of the Pl–To hiatus at Sancerre-Couy as large uncertainties remain on the ages of Lower Jurassic ammonite zones and subzones.

6. Conclusions

This study allows us to draw the following conclusions:

(1) The ammonite zonation of the Sancerre-Couy core is revised for the upper Sinemurian to lowermost Toarcian interval and a new comprehensive record has been presented.

(2) The calcareous nannofossil assemblage of the Sancerre-Couy core contains a mixed assemblage of species with Mediterranean and (sub-) boreal affinities allowing the application and correlation of both standard schemes.

(3) Relative sea-level changes have had a great influence on calcareous nannofossil biostratigraphy of the Sancerre-Couy core with the FCO of coccoliths related to a major transgression in the mid-Sinemurian. Studies of Sinemurian material from more distal, hemipelagic sites are greatly needed to improve the biostratigraphy and better document evolutionary steps of calcareous nannofossils in that interval.

(4) The high sampling density used in this study reveals that FOs and LOs of well-established biostratigraphic markers do not systematically appear as robust and reliable bioevents. The low abundance of many species toward the base and top of their range lead to inconsistent occurrences and the distinction of potentially more reliable FCOs and LCOs that should be thoroughly tested in the different oceanic domains throughout the Lower Jurassic.

(5) The calibration of the nannofossil biozonations and secondary bioevents at Sancerre-Couy to ammonite biostratigraphy allowed comparison to other oceanic basins and a detailed review of potentially synchronous and time-transgressive bioevents. A number of reliable secondary bioevents, not currently used in standard biostratigraphic schemes, appear useful for large-scale correlations.

(6) Ammonite and calcareous nannofossil biostratigraphy are calibrated to a new high-resolution organic carbon isotope curve that reveals a number of useful negative and positive excursions throughout the Sinemurian–Pliensbachian interval.

(7) The biostratigraphy and carbon-isotope stratigraphy of Sancerre-Couy, together with sedimentary features, reveal a large number of hiatuses and/or condensed intervals in the core throughout the Sinemurian to lowermost Toarcian, which is consistent with high amplitude rapid relative sea-level changes associated to tectonics and potential greenhouse-icehouse climatic changes.

Acknowledgements

We thank Ángela Fraguas and Emanuela Mattioli for fruitful discussions on calcareous nannofossil taxonomy and Inge Juul, Anne Thoisen and Bo Petersen for assistance in the lab. Many thanks to Jacqueline Lorenz for her precious help sending out all her original working documents on the Sancerre-Couy core. Olivier Serrano and Pierrick Graviou are warmly thanked for their help at the core storage of the BRGM. We thank the editor and two anonymous reviewers for their helpful comments, which have strongly improved an earlier version of this manuscript.

References

Armendariz, M., Rosales, I., Bádenas, B., Aurell, M., García-Ramos, J.C., Piñuela, L., 2012. High-resolution chemostratigraphic records from Lower Pliensbachian belemnites: Palaeoclimatic perturbations, organic facies and water mass exchange (Asturian basin, northern Spain). Palaeogeography, Palaeoclimatology, Palaeoecology 333-334, 178-191.

Bartolini, A., Guex, J., Spangenberg, J.E., Schoene, B., Taylor, D.G., Schaltegger, U., Atudorei, V., 2012. Disentangling the Hettangian carbon isotope record: Implications for the aftermath of the end-Triassic mass extinction. Geochemistry Geophysics Geosystems 13 (1), 1-11. doi:10.1029/2011GC003807.

Bassoulet, J.P., Baudin, F., 1994. Le Toarcien inférieur: un épisode de crise dans les bassins et sur les plates-formes carbonatées de l'Europe du Nord-Ouest et de la Téthys. Geobios 17, 645-654.

Bassoulet, J.P., Elmi, S., Poisson, A., Cecca, F., Bellion, Y., Guiraud, R., Baudin, F., 1993. Middle Toarcian (184-182 Ma). In: Dercourt, J., Ricou, L.E., Vrielynck, B. (Eds.), Atlas Tethys Paleoenvironmental Maps. Explanatory notes. Gauthiers-Villards, Paris, 63-80.

Baudin, F., Herbin, J-P, Vandenbroucke, M., 1990. Mapping and geochemical characterization of the Toarcian organic matter in the Mediterranean Tethys and Middle East. Organic Geochemistry 16 (4-6), 677-687.

Bordiga, M., Bartol, M., Henderiks, J., 2015. Absolute nannofossil abundance estimates: Quantifying the pros and cons of different techniques. Revue de Micropaléontologie 58 (3), 155-165. doi: 10.1016/j.revmic.2015.05.002.

Bour, I., Mattioli, E., Pittet, B., 2007. Nannofacies analysis as a tool to reconstruct paleoenvironmental changes during the Early Toarcian anoxic event. Palaeogeography, Palaeoclimatology, Palaeoecology 249, 58-79.

Bucefalo Palliani, R., Cirilli, S., Mattioli, E., 1998. Phytoplankton response and geochemical evidence of the lower Toarcian relative sea level rise in the Umbria-Marche basin (Central Italy). Palaeogeography, Palaeoclimatology, Palaeoecology 142, 33-50.

Bucefalo Palliani, R., Mattioli, E., Riding, J.B., 2002. The response of marine phytoplankton and sedimentary organic matter to the early Toarcian (Lower Jurassic) oceanic anoxic event in northern England. Marine Microplaeontology 46, 223-245.

Boulila, S., Galbrun, B., Huret, E., Hinnov, L.A., Rouget, I., Gardin, S., Bartolini, A., 2014. Astronomical calibration of the Toarcian Stage: Implications for sequence

stratigraphy and duration of the early Toarcian OAE. Earth and Planetary Science Letters 386, 98-111. doi: 10.1016/j.epsl.2013.10.047.

Bown, P.R., 1987. Taxonomy, evolution, and biostratigraphy of Late Triassic–Early Jurassic calcareous nannofossils. Special Paper Palaeontology 38, 1-118.

Bown, P.R., Cooper, M.K.E., 1998. Jurassic. In: Bown, P.R. (Ed.), Calcareous Nannofossil Biostratigraphy. British Micropalaeontological Society Series. Chapman and Hall/Kluwer Academic Publishers, London, 86-131.

Bown, P.R., Lees, J.A., Young, J.R., 2004. Calcareous nannoplankton evolution and diversity through time. In: Thierstein, H.R., Young, J.R. (Eds.), Coccolithophores from Molecular Processes to Global Impact. Springer, Amsterdam, 481-508.

Clémence, M.-E., Gardin, S., Bartolini, A., 2015. New insights in the pattern and timing of the Early Jurassic calcareous nannofossil crisis. Palaeogeography, Palaeoclimatology, Palaeoecology 427, 100-108. doi: 10.1016/j.palaeo.2015.03.024.Degouy, M., Lorenz, C., Michaely, B., Megnien, C., Weber, C., 1986. Rapport d'activité du forage de Sancerre-Couy (cher) – Novembre 1986 – Troisième phase d'investigation GPF 3, Rapport interne du Bureau de recherches géologiques et minières (BRGM) 86 SGN 695 GEO, Orléans, 13 p.

Dera, G., Brigaud, B., Monna, F., Laffont, R., Pucéat, E., Deconinck, J.-F., Pellenard, P., Joachimski, M. M., Durlet, C., 2011. Climatic ups and downs in a disturbed Jurassic world. Geology 39, 215-218. doi: 10.1130/G31579.1.

Dommergues, J.-L. and Mouterde, R. 1981. Les acanthopleurocératinés portugais et leurs relations avec les formes sbuboréales. Ciências da Terra 6, 77-100.

de Kænel, E., Bergen, J.A., 1993. New Early and Middle Jurassic coccolith taxa and biostratigraphy from the eastern proto-Atlantic (Morocco, Portugal and DSDP Site 547 B). Eclogae Geologicae Helvetiae 86 (3), 861-908.

Duarte, L.V., Comas-Rengifo, M.J., Silva, R.L., Paredes, R., Goy, A., 2014. Carbon isotope stratigraphy and ammonite biochronostratigraphy across the Sinemurian–Pliensbachian boundary in the western Iberian margin. Bulletin of Geosciences 89 (4), 719-736. doi: 10.3140/bull.geosci.1476.

Erba, E., 2006. The first 150 million years history of calcareous nannoplankton: Biospehere-geosphere interactions. Palaeogeography, Palaeoclimatology, Plaeoecology 232, 237-250. doi:10.1016/j.palaeo.2005.09.013.

Fraguas, Á., Erba, E., 2010. Biometric analyses as a tool for the differentiation of two coccolith species of the genus Crepidolithus (Pliensbachian, Lower Jurassic) in the Basque-Cantabrian Basin (Northern Spain). Marine Micropaleontology 77, 125-136.

Fraguas, Á., Young, J.R., 2011. Evolution of the coccolith genus Lotharingius during the Late Pliensbachian–Early Toarcian interval in Asturias (N Spain). Consequences of the Early Toarcian environmental perturbations. Geobios 44, 361-375. doi:10.1016/j.geobios.2010.10.005.

Fraguas, Á., Comas-Rengifo, M.J., Perilli, N., 2008. Pliensbachian calcareous nannofossils of the Santotis Section (Basque-Cantabrian Basin, N Spain). Atti della Societa Toscana di Scienze Naturali, Memorie Serie A 113, 49-56.

Fraguas, Á., Comas-Rengifo, M.J., Gómex, J.J., Goy, A., 2012. The calcareous nannofossil crisis in Northern Spain (Asturias province) linked to the Early Toarcian warming-driven mass extinction. Marine Micropaleontology 94-95, 58-71.

Fraguas, Á., Comas-Rengifo, M.J., Perilli, N., 2015. Calcareous nannofossil biostratigraphy of the Lower Jurassic in the Cantabrian Range (Northern Spain). Newsletters on Stratigraphy 48 (2), 179-199. doi: 10.1127/nos/2015/0059.

Fraguas, Á., Comas-Rengifo, M.J., Perilli, N., 2016. Erratum to "Calcareous nannofossil biostratigraphy of the Lower Jurassic in the Cantabrian Range (Northern Spain)" (Newsletter on Stratigraphy 48/2 (2015), 179-199). Newsletters on Stratigraphy 49 (1), 69–70. doi: 10.1127/nos/2015/0070.

Franceschi, M., Dal Corso, J., Posenato, R., Roghi, G., Masetti, D., Jenkyns, H.C., 2014. Early Pliensbachian (Early Jurassic) C-isotope perturbation and the diffusion of the Lithiotis Fauna: Insights from the western Tethys. Palaeogeography, Palaeoclimatology, Palaeoecology 410, 255-263.

Gardin, S., Krystyn, L., Richoz, S., Bartolini, A., Galbrun, B., 2012. Where and when the earliest coccolithophores? Lethaia 45, 507-523.

Gély, J.-P., Lorenz, J., 1991. Analyse séquentielle du Jurassique (Hettangien á Callovien) du sondage de Couy (Bassin Parisien). Comptes Rendus de l'Académie des Sciences Paris 313 (Série II), 347-353.

Gomez, J.J., Comas-Rengifo, M.J., Goy, A., 2016. Palaeoclimatic oscillations in the Pliensbachian (Early Jurassic) of the Asturian Basin (Northern Spain). Climate of the Past 12, 1199-1214. doi: 10.5194/cp-12-1199-2016.

Hallam, A., 1997. Estimates of the amount and rate of sea-level changes across the Rhaetian-Hettangian and Pliensbachian-Toarcian boundaries (Latest Triassic to Early Jurassic). Journal of the Geological Society London, 154 (773-779). doi:10.1144/gsjgs.154.5.0773.

Hermoso, M., Le Callonnec, L., Minoletti, F., Renard, M., Hesselbo, S.P., 2009. Expression of the Early Toarcian negative carbon-isotope excursion in separated carbonate microfractions (Jurassic, Paris Basin). Earth and Planetary Science Letters 277, 194-203. doi:10.1016/j.epsl.2008.10.013.

Hermoso, M., Minoletti, F., Pellenard, P., 2013. Black shale deposition during Toarcian super-greenhouse driven by sea level. Climate of the Past 9, 2703-2712. doi:10.5194/cp-9-2703-2013.

Hesselbo S.P., Grocke D.R., Jenkyns H.C., Bjerrum C.J., Farrimond P., Morgans Bell H.S., Green O.R., 2000. Massive dissociation of gas hydrate during a Jurassic oceanic anoxic event. Nature 406 (6794), 392-395. doi:10.1038/35019044.

Hesselbo S.P., Jenkyns H.C., Duarte L.V., Veiga de Oliveira L.C., 2007. Carbon-isotope record of the Early Jurassic (Toarcian) Oceanic Anoxic Event from fossil wood and marine carbonate (Lusitanian Basin, Portugal). Earth and Planetary Science Letters 253 (3-4), 455-470. doi:10.1016/j.epsl.2006.11.009.

Howarth, M.K., 1992. The ammonite family Hildoceratidae in the Lower Jurassic of Britain. Part 1. Monograph of the Palaeontographical Society London: pp. 1-106, pl. 1-16 Publ. No. 586, part of vol. 146 for 1991; Part 2: 107-200, pl. 17-38 Publ. No. 590, part of vol. 146 for 1992, 1992.

Jenkyns, H.C., 1988. The early Toarcian (Jurassic) anoxic event: Stratigraphic, Sedimentary, and Geochemical Evidence. American Journal of Science 288, 101-151.

Jenkyns, H.C., Weedon, G.P., 2013. Chemostratigraphy (CaCO3, TOC, δ13Corg) of Sinemurian (Lower Jurassic) black shales from the Wessex Basin, Dorset and palaeoenvironmental implications. Newsl.Stratigr.46(1),1–21.Koch, C., Young, J.R., 2007. A simple weighing and dilution technique for determining absolute abundances of coccoliths from sediment samples. Journal of Nannoplankton Research 29 (1), 67-69.

Korte, C., Hesselbo, S.P., 2011. Shallow marine and oxygen isotope and elemental records indicate icehouse-greenhouse cycles during the Early Jurassic. Paleoceanography 26, PA4219, 1-18. doi:10.1029/2011PA002160.

Littler, K., Hesselbo, S.P., Jenkyns, H.C., 2010. A carbon-isotope perturbation at the Pliensbachian-Toarcian boundary: evidence from the Lias Group, NE England. Geological Magazine 147 (2), 181-192. doi: 10.1017/S0016756809990458.

Lorenz, C., 1987. Forage scientifique de Sancerre-Couy (Cher). Rapport d'exécution et descriptions préliminaires. Terrains sédimentaires. Documents du Bureau Recherches Géologiques et Minières Paris 136, 205 p.

Lorenz, C., Gély, J.P., 1994. Interprétation séquentielle du Jurassique inférieur et moyen du Sud du Bassin Parisien à partir des corrélations diagraphiques calées sur le forage de Couy (Cher, France). [Sequence analysis from Lower and Middle Jurassic of the South of Paris Basin well-log correlated to the Couy borehole (Cher, France)]. Geobios M.S. 17, 597-604.

Lorenz, J., Lefavrais, A., Depeche, F., Leclerc, V., Marchand, D., Roy, B., Taugourdeau, J., Reyre, Y., 1987. Le Jurassique. In: Lorenz, C. (Ed.), Forage scientifique de Sancerre-Couy (Cher). In: Documents du Bureau de Recherches Géologiques et Minières 136. Bureau de Recherches Géologiques et Minières, 19-26.

Lorenz, J., Delavenna, M.F., Holtzapffel, T., Lefavrais, A., Trauth, N., Steinberg, M., 1988. Biostratigraphie, lithologie et minéralogie du Lias et du Dogger traversés par le forage profond "Anomalie magnétique du Bassin de Paris" Programme Gélogie profonde de la France. 2nd International Symposium on Jurassic Stratigraphy Lisbonne, 947-961.

Lorenz, C., Lefavrais, A., Lorenz, J., Marchand, D., Millon, R., 1991. Calage stratigraphique des diagraphies du Jurassique du sud du Bassin parisien à partir du sondage de Sancerre-Couy (programme profond Géologie profonde de la France). Bulletin de la Société Géologique de France 162, 947-952.

Mailliot, S., Mattioli, E., Guex, J., Pittet, B., 2006. The Early Toarcian anoxia, a synchronous event in the Western Tethys? An approach by quantitative biochronology (Unitary Associations), applied on calcareous nannofossils. Palaeogeography, Palaeoclimatology, Palaeoecology 240 (3), 562-586.

Mailliot, S., Elmi, S., Mattioli, E., Pittet, B., 2007. Calcareous nannofossil assemblages across the Pliensbachian/Toarcian boundary at the Peniche section (Ponta do Trovão, Lusitanian Basin). Ciências da Terra 16, 51-62.

Mailliot, S., Mattioli, E,, Bartolini, A., Baudin, F., Pittet, B., Guex, J., 2009. Late Pliensbachian-Early Toarcian (Early Jurassic) environmental changes in an epicontinental basin of NW Europe (Causses area, central France): A micropaleontological and geochemical approach. Palaeogeography, Palaeoclimatology, Palaeoecology 273, 346-364.

Martinez, M., Dera, G., 2015 Orbital pacing of carbon fluxes by a ~9-My eccentricity cycle during the Mesozoic. PNAS 112 (41), 12604-12609. doi: 10.1073/pnas.1419946112.

Mattioli, E., 1996. New Calcareous Nannofossil species from the Early Jurassic of Tethys. Rivista Italiana di Paleontologia e Stratigrafia 102 (3), 397-412.

Mattioli, E., Erba, E., 1999. Synthesis of calcareous nannofossil events in the Tethyan Jurassic. Rivista Italiana di Paleontologia e Stratigrafia 105 (3), 343-376.

Mattioli, E., Pittet, B., Bucefalo Palliani, R., Röhl, H.-J., Schmid-Röhl, A., Morettini, E., 2004a. Phytoplankton evidence for the timing and correlation of palaeoceanographical changes during the early Toarcian oceanic anoxic event (Early Jurassic). Journal of the Geological Society London 161, 685-693.

Mattioli, E., Pittet, B., Young, J.R, Bown, P.R., 2004b. Biometric analysis of Pliensbachian – Toarcian (Lower Jurassic) coccoliths of the family Biscutaceae: intra- and interspecific variability versus palaeoenvironmental influence. Marine Micropaleontology 52, 5-27. doi:10.1016/j.marmicro.2004.04.004.

Mattioli, E., Pittet, B., Suan, G., Mailliot, S., 2008. Calcareous nannoplankton changes across the Early Toarcian oceanic anoxic event in the western Tethys. Paleoceanography 23, PA3208, 1-17. doi:10.1029/2007PA001435.

Mattioli, E., Pittet, B., Petitpierre, L., Mailliot, S., 2009. Dramatic decrease of pelagic carbonate production by nannoplankton across the Early Toarcian anoxic event (T-OAE). Global and Planetary Change 65, 134-145.

Mattioli, E., Plancq, J., Boussaha, M., Duarte, L.V., Pittet, B., 2013. Calcareous nannofossil biostratigraphy: new data from the Lower Jurassic of the Lusitanian Basin. Comunicações Geológicas 100, 69-76 (Especial I).

Morettini, E., Santantonio, M., Bartolini, A., Cecca, F., Baumgartner, P.O., Hunziker, J.C., 2002. Carbon isotope stratigraphy and carbonate production during the Early-Middle Jurassic: examples from the Umbria-Marche-Sabina Apennines (central Italy). Palaeogeography, Palaeoclimatology, Palaeoecology 184, 251-273.

Müller, T., Price, G.D., Bajnai, D, Nyerges, A., Kesjar, D, Raucsik, B., Varga, A., Judik, K., Fekete, J., May, Z., Pálfy, J., 2016. New multiproxy record of the Jenkyns Event (also known as the Toarcian Oceanic Anoxic Event) from the Mecsek Mountains (Hungary): Differences, duration and drivers. Sedimentology, in press, doi: 10.1111/sed.12332.

Page, K.N., 2003. The Lower Jurassic of Europe: its subdivision and correlation. Geological Survey of Denmark and Greenland Bulletin 1, 23–59.

Perch-Nielsen, K., 1985. Mesozoic Calcareous Nannofossils. In: Bolli, H.M., Saunders, J.B., Perch-Nielsen, K. (Eds.), Plankton Stratigraphy. Cambridge University Press, Cambridge, 329-426.

Perilli, N., 2000. Calibration of early–middle Toarcian nannofossil events based on high-resolution ammonite biostratigraphy in two expanded sections from the Iberian Range (East Spain). Marine Micropaleontology 39, 293-308.

Perilli, N., Fraguas, A., Comas-Rengifo, M.J., 2010. Reproducibility and reliability of the Pliensbachian calcareous nannofossil biohorizons from the Basque-Cantabrian Basin (Northern Spain). Geobios 43, 77-85. doi:10.1016/j.geobios.2009.06.009.

Pittet, B., Suan, G., Lenoir, F., Duarte, L.V., Mattioli, E., 2014. Carbon isotope evidence for sedimentary discontinuities in the lower Toarcian of the Lusitanian Basin (Portugal): Sea level change at the onset of Oceanic Anoxic Event. Sedimentary Geology 303, 1-14.

Plancq, J., Mattioli, E., Pittet, B., Baudin, F., Duarte, L.V., Boussaha, M., Grossi, V., 2016. A calcareous nannofossil and organic geochemical study of marine palaeoenvironmental changes across the Sinemurian/Pliensbachian (early Jurassic, ~191 Ma) in Portugal. Palaeogeography, Palaeoclimatology, Palaeoecology 449, 1-12.

Porter, S.J., Smith, P.L., Caruthers, A.H., Hou, P., Gröcke, D.R., Selby, D., 2014. New high resolution geochemistry of Lower Jurassic marine sections in western North America: A global positive carbon isotope excursion in the Sinemurian ? Earth and Planetary Science Letters 397, 19–31.

Quesada, S., Robles, S., Rosales, I., 2005. Depositional architecture and transgressive-regressive cycles within Liassic backstepping carbonate ramps in the Basque-Cantabrian Basin, northern Spain. Journal Of The Geological Society London 162, 531-548.

Riding, J.B., Leng, M.J., Kender, S., Hesselbo, S.P., Feist-Burkhardt, S., 2013. Isotopic and palynological evidence for a new Early Jurassic environmental perturbation. Palaeogeography, Palaeoclimatology, Palaeoecology 374, 16-27. http://dx.doi.org/10.1016/j.palaeo.2012.10.019.

Rocha, R.B., Mattioli, E., Duarte, L.V., Pittet, B., Elmi, S., Mouterde, R., Cabral, M.C., Comas-Rengifo, M.J., Gómez, J.J., Goy, A., Hesselbo, S.P., Jenkyns, H.C., Littler, K., Mailliot, S., Veiga de Oliveira, C., Osete, M.L., Perilli, N., Pinto, S., Ruget, C., Suan, G., 2016. Base of the Toarcian Stage of the Lower Jurassic defined by the Global Boundary Stratotype Section and Point (GSSP) at the Peniche section (Portugal). Episodes 39, 460-481.

Roth, P.H., 1983. Jurassic and Lower Cretaceous calcareous nannofossils in the western North Atlantic (Site 543): biostratigraphy, preservation and some observations on biogeography and paleoceanography. Initial Reports of the Deep Sea Drilling Project 76, 587-621.

Röhl, H.-J., Schmid-Röhl, A., Oschmann, W., Frimmel, A., Schwark, L., 2001. The Posidonia Shale (Lower Toarcian) of SW-Germany: An oxygen-depleted ecosystem controlled by sea level and palaeoclimate. Palaeogeography, Palaeoclimatology, Palaeoecology 165, 27-52.

Ruebsam, W., Münzberger, P., Schwark, L., 2014. Chronology of the Early Toarcian environmental crisis in the Lorraine Sub-Basin (NE Paris Basin). Earth and Planetary Science Letters 404, 273-282.

Ruhl, M., Deenen, M.H.L., Abels, H.A., Bonis, N.R., Krijgsman, W., Kürschner, W.M., 2010. Astronomical constraints on the duration oft he early Jurassic Hettangian stage and recovery rates following the end-Triassic mass extinction (St Audrie's Bay/East Quantoxhead, UK). Earth and Planetary Science Letters 295, 262-276. doi: 10.1016/j.epsl.2010.04.008.

Sapunov, I.G., Metodiev, L.S., 2007. The Hettangian-Pliensbachian ammonite zones and subzones in Bulgaria – a retrospection and correlation with the standard zones and subzones in North-western Europe. Comptes rendus de l'Académie bulgare des Sciences 60, 991-1000.

Silva, R.L., Duarte, L.V., Comas-Rengifo, M.J., Mendonça Filho, J.G., Azerêdo, A.C., 2011. Update of the carbon and oxygen isotopic records of the Early-Late Pliensbachian (Early Jurassic, ~187 Ma): Insights from the organic-rich hemipelagic series of the Lusitanian Basin (Portugal). Chemical Geology 283, 177-184. doi: 10.1016/j.chemgeo.2011.01.010.

Silva, R.L. and Duarte, L.V. 2015. Organic matter production and preservation in the Lusitanian Basin (Portugal) and Pliensbachian climatic hot snaps. Global and Planetary Change 131, 24-34. doi: 10.1016/j.gloplacha.2015.05.002.

Suan, G., Mattioli, E., Pittet, B., Mailliot, S., Lécuyer, C., 2008, Evidence for major environmental perturbation prior and during the Toarcian (Early Jurassic) oceanic anoxic event from the Lusitanian Basin, Portugal. Paleoceanography 23, PA1202. doi: 10.1029/2007PA001459.

Suan, G., Mattioli, E., Pittet, B., Lécuyer, C., Suchéras-Marx, B., Duarte, L.V., Philippe, M., Reggiani, L., Martineau, F., 2010. Secular environmental precursors to Early Toarcian (Jurassic) extreme climate changes. Earth and Planetary Science Letters 290, 448-458.

Suan, G., van de Schootbrugge, B., Adatte, T., Fiebig, J., Oschmann, W., 2015. Calibrating the magnitude of the Toarcian carbon cycle perturbation. Paleoceanography 30, 495-509. doi: 10.1002/2014PA002758.

Thibault, N., Harlou, R., Schovsbo, N., Schiøler, P., Minoletti, F., Galbrun, B., Lauridsen, B.W., Sheldon, E., Stemmerik, L., Surlyk, F., 2012. Upper Campanian-Maastrichtian nannofossil biostratigraphy and high-resolution carbon-isotope stratigraphy of the Danish Basin: Towards a standard δ13C curve for the Boreal Realm. Cretaceous Research 33, 72-90. doi:10.1016/j.cretres.2011.09.001.

Thibault, N., Anderskouv, K., Bjerager, M., Boldreel, L.O., Jelby, M.E., Stemmerik, L., Surlyk, F., 2015. Upper Campanian–Maastrichtian chronostratigraphy of the Skælskør-1 core, Denmark: correlation at the basinal and global scale and implications for changes in sea-surface temperatues. Lethaia 48 (4), 549-560. doi: 10.1111/let.12128.

Tremolada, F., Van de Schootbrugge, B., Erba, E., 2005. Early Jurassic schizosphaerellid crisis in Cantabria, Spain: Implications for calcification rates and phytoplankton evolution across the Toarcian oceanic anoxic event. Paleoceanography 20 (2), PA2011. doi: 10.1029/2004PA001120.

van de Schootbrugge, B., Bailey, T.R., Rosenthal, Y., Katz, M.E., Wright, J.D., Miller, K.G., Feist-Burkhardt, S., Falkowski, P.G., 2005. Early Jurassic climate change and the radiation of organic-walled phytoplankton in the Tethys Ocean. Paleobiology 31 (1), 73-97.

van de Schootbrugge, B., Payne, J.L., Tomasovych, A., Pross, J., Fiebig, J., Benbrahim, M., Föllmi, K.B., Quan, T.M., 2008. Carbon cycle perturbation and stabilization in the wake of the Triassic-Jurassic boundary mass-extinction event. Geochemistry, Geophysics, Geosystems 9 (4), 1-16. doi: 10.1029/2007GC001914.

Veiga de Oliveira, L.C., Rodrigues, R., Duarte, L.V., Lemos, V.B., 2006. Avaliação do potencial gerador de petróleo e interpretação paleoambiental com base em biomarcadores e isótopos estáveis de carbono da seção Pliensbaquiano-Toarciano inferior (Jurássico Inferior) da região de Peniche (Bacia Lusitânica, Portugal). Assessment of oil generation potential and paleoenvironment using biomarkers and stable carbon isotopes, Pliensbachian-lower Toarcian (Lower Jurassic) section at Peniche (Lusitanian Basin, Portugal). Boletim de GeociEncias da Petrobras 14 (2), 207-234.

Veiga de Oliveira, L.C., Perilli, N., Duarte, L.V., 2007. Calcareous nannofossil assemblages around the Pliensbachian/Toarcian boundary in the reference section of Peniche (Portugal). Ciências da Terra 16, 45-50.